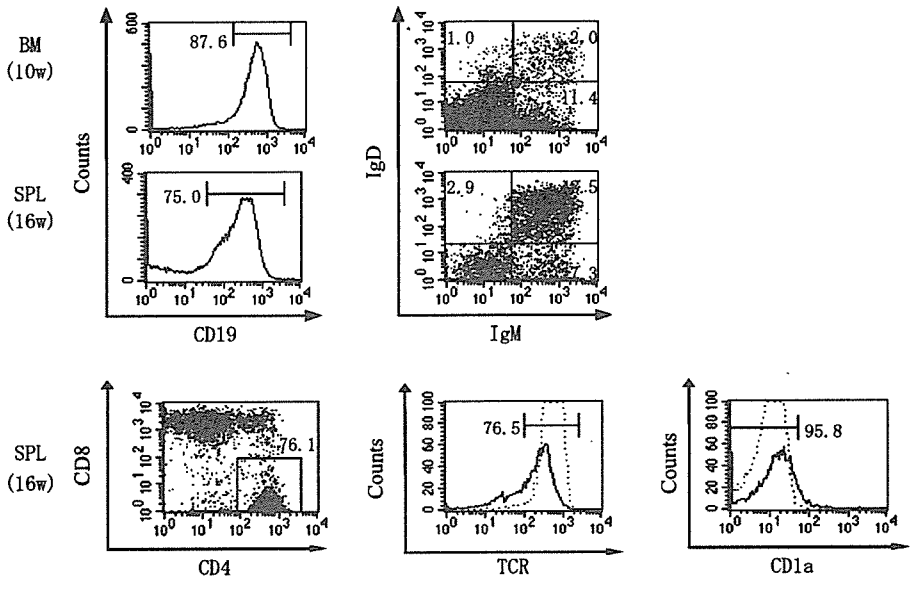

Figure 1. Reconstitution of human immune system in nonobese diabetic/severe combined immunodeficient/gammac(null) mouse with umbilical cord blood $CD34^+$ cells. Fluorescein-activated cell sorting analysis of lymphoid tissue cells. Bone marrow (BM) cells were prepared 10 weeks after transplantation. Spleen (SPL) cells were prepared 16 weeks after transplantation. CD4SP cells were enclosed in a square and the percentage was shown above the square. T-cell receptor (TCR) and CD1a expression was analyzed for the CD4SP-gated fractions. B cells were gated for $CD19^+$ cells, and immunoglobulin (Ig) IgM and IgD double-staining patterns are shown.

Results

CB-NOG can produce specific antibodies against ordinary protein antigens

We reported previously that IgM+IgD+mature type human B cells are detectable in the spleen and bone marrow of NOG mouse reconstituted with CB-derived $CD34^+$ cells (CB-NOG mouse), although the majority of IgM^+ cells in bone marrow are IgD-negative immature B cells [12]. In addition, as shown in Figure 1 of this study, the spleen of these CB-NOG mice were shown to contain CD4 and CD8 single-positive human T cells, with high expression of TCR. The pattern of mature T and B cells as shown in Figure 1 was observed in the mice with relatively high reconstitution ratio of human-derived cells (>20%, data not shown). Thus, for examination of human antibody production specific to a given antigen, we used CB-NOG mice, the engraftment of which was >20% in the 8th to 10th week after transplantation of human CB cells. These CB-NOG mice were immunized with Her-2 extracellular domain (exHer-2), DNP-KLH as a hapten-carrier system, or whole protein TSST-1 intraperitoneally with alum biweekly (Fig. 2A). Two experiments were performed using CB-NOG mouse groups, each of which was transplanted with one-donor–derived $CD34^+$ cells (Table 1).

Antigen-specific IgM was detected in the sera of mice immunized with three kinds of antigens in both experiments, but specific IgG was not detected even after five boosters in all CB-NOG mice (data not shown). Reconstitution efficiency, which was determined by the proportion of human $CD45^+$ cells in the peripheral blood and specific IgM producibility were not statistically correlated in the immunized mice (Fig. 2B). Moreover, the immunized CB-NOG mouse showed very little positive correlation between total serum IgM and specific IgM producibility (Fig. 2C). Among the immunized mice with each protein antigen, the ratio of mice producing specific antibody against exHer-2 was lower (3/6) in comparison with that of mice immunized with DNP-KLH (4/4) and TSST-1 (2/2 in experiment 1 and 7/11 in experiment 2) (Table 1).

Detection of human IgM antibody specific for Her-2-peptide antigen

We have previously reported on the preparation of a humanized antibody termed CH401, which recognizes extracellular domain of Her-2 different from the recognition site of Herceptin [19]. Moreover, we recently identified an epitope peptide recognized by CH401 (Miyako et al., manuscript in preparation). In consideration of the clinical application of oligo-clonal antibodies carrying various epitopes, such epitope-specific antibodies would be useful. Then, we tried to raise the specific IgM antibody against an epitope peptide of CH401 in the immunized CB-NOG mice based on the above result that CB-NOG mice can produce human-derived IgM antibodies specific for the immunized exHer-2 protein antigen. However, because Her-2 is originally a membrane protein, the question remained whether immunization of a Her-2–derived peptide could promote production of antibodies against the CH401 epitope peptide (20 amino residues), which recognize Her-2 whole chain expressed on the cell surface. For that, we examined whether immunization of the peptide alone can induce efficiently specific antibody

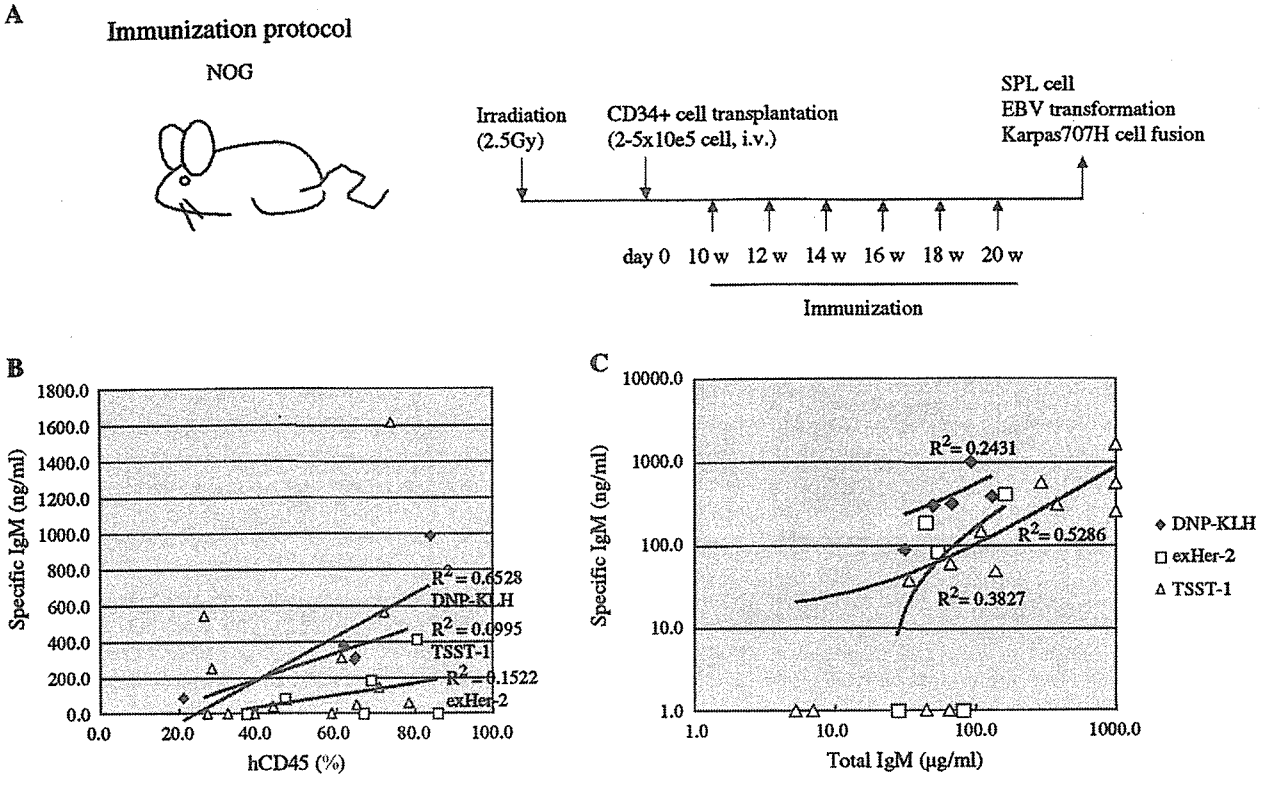

Figure 2. Correlation of specific antibody with reconstitution efficiency. (A) Nine-week-old nonobese diabetic/severe combined immunodeficient/ gammac(null) (NOG) mice were irradiated and transplanted with $CD34^+$ cells purified from cord blood. Ten weeks after the transplantation, immunization was started biweekly. Four days after the last booster, splenocytes were prepared and fused with Karpas707H. (B) Specific immunoglobulin M (IgM) of the mice vs hCD45 (%) of the mice for experiment 1 data. $R^2 = 0.6528$ for 2,4-dinitrophenol-conjugated keyhole-limpet-hemocyanin (DNP-KLH), $R^2 = 0.1522$ for exHer-2, $R^2 = 0.0995$ for toxic shock syndrome toxin-1 (TSST-1). Totally not so high correlation between the concentration of specific antibodies and efficiency of engraftment was observed. (C) Specific IgM/total IgM were analyzed for experiment 1 data shown in Table 1. Samples with specific antibodies were used for estimating the coefficients of correlation. $R^2 = 0.2431$ for DNP-KLH, $R^2 = 0.3827$ for Her-2, $R^2 = 0.5286$ for TSST-1.

production or whether co-immunization with cells expressing Her-2 on their surface provides synergistic or additional effect on anti-peptide antibody production. An immunization protocol we performed was shown in Figure 2A and Table 2. For peptide immunization, we used MAP because MAP peptides were reported to have similar immunogenicities to hapten-carrier antigens [20,21].

Ten and 20 weeks after $CD34^+$ cell transplantation (pre-immunization and a week after the fifth immunization), sera were collected and ELISA was performed for measuring serum level of anti-peptide antibodies (Table 3). In experiment 2-1, 16 NOG mice transplanted with human CB cells obtained from one donor were divided into three groups and immunized with epitope peptide alone (P), SV22, a NIH3T3-derived cell line expressing Her-2 (S), or epitope peptide plus SV22 (P/S), respectively. Peptide-specific IgM antibody was substantially detectable in 2/3 CB-NOG mice receiving epitope peptide alone. In comparison, immunization of SV22 or of SV22 plus epitope peptide led the ratio of anti-peptide–producing mice to 100%. The similar tendency was found in experiment 2-2, in which CB-NOG mice received another donor-derived $CD34^+$ CB cells. These results showed that a peptide immunization is capable of producing the peptide-specific antibody in CB-NOG mice. Although the ratio of antibody-producing mice was higher in mice immunized with SV22 cells plus peptide than in mice immunized with peptide alone, the same high efficiency was also found with immunization with SV22 cells, suggesting that the Her-2 epitope has sufficient antigenicity in the whole Her-2 molecule on the cell surface without additional immunization with the peptide.

Human hybridoma preparation using human myeloma cell line Karpas707H

Next, we tried to establish human–human hybridoma by fusing B cells prepared from the spleen of immunized CB-NOG mouse with a human myeloma cell line. As for human myeloma cell line, Karpas707H was used. Specificity of antibodies secreted in the culture supernatant was analyzed by ELISA, results of which are shown in Table 4. Only four Her-2–specific hybridoma lines were obtained from the mice immunized with exHer-2, while 32 hybridoma lines were obtained for DNP-KLH specific B cells. As CB-NOG mice produce mainly IgM isotype for antigen-specific antibody, spleen cells of the mice immunized with Her-2 peptide and SV22 were transformed with EBV before the fusion with

Table 1. Summary of specific antibody production in CB-NOG

Ag	Total IgM (μg/mL)	hCD45 (%)	Specific IgM (ng/mL)
	Experiment 1-1		
DNP-KLH	131.9	62.0	375.3
DNP-KLH	93.4	84.1	981.8
DNP-KLH	50.2	64.8	294.7
DNP-KLH	31.9	21.4	86.0
exHer-2	162.8	80.7	409.5
exHer-2	110.7	37.4	0.0
exHer-2	54.1	47.0	81.8
exHer-2	44.7	69.0	182.5
exHer-2	28.5	67.1	0.0
exHer-2	82.2	86.0	0.0
TSST-1	139.2	65.3	47.9
TSST-1	34.2	44.1	36.8
	Experiment 1-2		
TSST-1	>1000	26.6	543.1
TSST-1	>1000	28.5	250.3
TSST-1	>1000	74.1	1610.4
TSST-1	110.1	71.1	143.4
TSST-1	295.8	72.4	561.0
TSST-1	381.3	61.5	305.3
TSST-1	65.9	59.0	0.0
TSST-1	45.2	32.7	0.0
TSST-1	67.1	78.7	58.5
TSST-1	5.3	27.4	0.0
TSST-1	7.0	39.5	0.0

Total immunoglobulin M (IgM), specific IgM, and percentage of human $CD45^+$ cells in bone marrow were compared. Percentage of $CD45^+$ cells was determined by fluorescein-activated cell sorting. Total and specific IgM levels were determined by enzyme-linked immunosorbent assay.
CB-NOG = NOG mouse reconstituted with CB-derived $CD34^+$ cells; DNP-KLH = 2,4-dinitrophenol-conjugated keyhole-limpet-hemocyanin; exHer-2 = Her-2 extracellular domain; TSST-1 = toxic shock syndrome toxin-1.

Karpas707H. As a result, we obtained specific antibody-producing hybridoma lines in both experiments, with or without EBV treatment. Consequently, totally 20 hybridoma lines producing peptide-specific antibody were obtained from the mice of experiment 2-1 (P/S-1, S and P/S-2). Moreover, 28 peptide-specific IgM-producing hybridoma lines were obtained in P/S-3 mice (experiment 2-2). One of these clones was expanded and anti-peptide IgM was collected from the supernatants. FACS analysis showed that the antibody specifically recognized surface Her-2 expressed on A20, though the intensity was not so high as that of Herceptin (Fig. 3). However, we could not detect any apoptotic effect of this antibody on Her-2–expressing cancer cells under the presence of human complement (data not shown).

These results suggest that NOG mice can produce antigen-specific IgM against very short epitope peptides. Antibody-producing B cells were successfully fused with a human myeloma cell line, and antibody-producing hybridoma was obtained. Using this system, we prepared hybridoma lines of completely human type secreting anti-Her-2 IgM.

Discussion

There is increasing evidence showing that clinical trials of certain humanized monoclonal antibodies are prospective [1,2], although their therapeutic effect is not always constitutive [22]. On the other hand, there is an argument that such antibodies may cause production of new anti-mouse antibodies during the continuous treatments because most of the therapeutic antibodies are generated from the human-mouse chimera antibody [8]. In this study, we examined the capacity of human B cells developed in mouse environment to produce antigen-specific antibodies, particularly against certain peptides, in vivo. For this, the human immune

Table 2. Immunization protocol for Her-2–related antigens

	Experiment 2-1				
	Immunization no.				
Group	1	2	3	4	5
1 (P)	Peptide	Peptide	Peptide	Peptide	Peptide
2 (P/S)	Peptide	Peptide	Peptide	SV22	SV22
3 (S)				SV22	SV22
	Experiment 2-2				
1 (P)	Peptide	Peptide	Peptide	Peptide	Peptide
2 (P/S)	Peptide	Peptide	Peptide	SV22	SV22
3 (H)	Her-2	Her-2	Her-2	Her-2	Her-2
4 (H/S)	Her-2	Her-2	Her-2	SV22	SV22
5 (S)				SV22	SV22

CB-NOG mice were immunized with Her-2–related antigens. In the experiment 2-1, epitope peptide and SV22 were used for the priming and booster. In the experiment 2-2, recombinant Her-2 extracellular domain protein (exHer-2) was also used.
CB-NOG = NOG mouse reconstituted with CB-derived $CD34^+$ cells; H = exHer-2; H/S = exHer-2 and SV22; P = peptide; P/S = peptide and SV22; S = SV22.

Table 3. Summary of anti-Her-2 antibody production in CB-NOG mice

	Experiment 2-1					
	10 Weeks after transplantation		20 Week after transplantation			
Ag	Total IgM (μg/mL)	hCD45 (%)	Total IgM (μg/mL)	Total IgG (ng/mL)	Her-2 IgM (ng/mL)	Anti-Peptide IgM (ng/mL)
P	90.7	81.4	287.9	13,548.9	0	334.4
P	58.2	30.8	418.6	2533.3	0	0
P	76.6	62.6	308.9	22,379.7	0	34.2
P/S	28	85.0	98.8	1237	18	138.4
P/S	153.7	82.1	373.4	55	0	65
P/S	104.9	88.3	185.6	26,855.3	0	59.2
P/S	94.1	83.7	250.2	0.361	0	53.6
P/S	98.2	63.8	228.2	10,788.9	0	60.7
P/S	123	63.0	208.4	0	0	52
P/S	7.6	51.8	96	0	3.6	50.4
P/S	55.7	45.5	368.3	0	0	37.6
P/S	325.1	64.5	424.8	0	0	111.2
P/S	133.6	71.1	166.9	0	0	106.9
S	47.5	72.8	194.8	801.2	0	153.7
S	108.6	61.8	324.1	4866.8	0	48.7
S	108.6	29.8	231	411.3	0	143.6
	Experiment 2-2					
P		88.3			0.0	0.0
P		80.5			0.0	0.0
P/S		83.0			0.0	5.0
P/S		57.1			0.0	12.5
P/S		90.1			0.0	0.0
P/S		39.5			725.9	613.8
H	ND	64.9	ND	ND	0.0	129.8
H		52.1			0.0	0.0
H		93.8			0.0	0.0
H		74.1			0.0	29.0
H/S		70.4			0.0	0.0
H/S		94.7			0.0	193.3
S		87.4			0.0	234.5
S		77.4			0.0	30.6

CB-NOG mice were immunized by the protocols as shown in Table 2. Total immunoglobulin M (IgM) and hCD45 (%) were determined 10 weeks after transplantation. Specific IgM, total IgM, and total IgG were determined at week 20.
CB-NOG = NOG mouse reconstituted with CB-derived $CD34^+$ cells; H = exHer-2; Her-2 = exHer-2 used for enzyme-linked immunosorbent assay (ELISA); H/S = exHer-2 and SV22; ND = not determined; P = peptide; Peptide = epitope peptide used for ELISA; P/S = peptide and SV22; S = SV22.

system in immunodeficient mouse was reconstituted by transplantation of human cord blood $CD34^+$ cells (CB-NOG), and they were thereafter immunized with given antigens. Then, antibody-producing human B cells obtained from the spleen of immunized CB-NOG mice were fused with a human myeloma cell line, which was recently established by Karpas et al. [18] to generate human–human hybridoma.

Among immunodeficient mice used for transplantation of human tissues, NOG mice were reported to be the most acceptable for human leukocytes [11]. Moreover, several groups including us showed that the human immune system could be efficiently reconstituted in NOG mice after transplantation of $CD34^+$ human cord blood cells [10,12,23,24]. Moreover, we demonstrated that the CB-NOG mice produced the antigen-specific antibody when they were immunized with DNP-KLH [12]. In this study, we examined whether peptide-specific antibodies are produced in the reconstituted CB-NOG mice when they were immunized with a MAP peptide with a small region of the Her-2 epitope peptide in Freund's complete adjuvant. In these mice, IgM production against a given short peptide antigen was detected with a relatively high frequency, which was not different from that of mice immunized with the ordinary protein antigens, such as a Her-2 extracellular domain. Compared with the peptide immunization, tumor cells expressing Her-2 on their surface induced anti-Her-2 peptide antibody production in a markedly high frequency. Peptide immunization did not have additive effect on the specific antibody induction when the Her-2–expressing cells were used for the antigen, as the frequency of antibody-producing mice and the antibody concentration in the sera were

Table 4. Summary of hybridoma production by CB-NOG B cells and Karpas707H

Ag	Mouse[a]	EBV	Cell[b] (x10e5)	Colony (n)	Total antibody (colony, n)		Specific antibody (colony, n)	
					IgM	IgG	IgM	IgG
H	4	–	921	142	21	15	4	ND
P/S-1	1	+	366	31	ND	ND	8	ND
P/S-2	1	+	255	14	ND	ND	2	ND
P/S-3	1	+	641	54	ND	ND	28	ND
S	1	+	358	48	ND	ND	10	ND
DNP-KLH	4	–	351	58	32	0	32	0

CB-NOG B cells were fused with Karpas707H and the yield was shown.
CB-NOG = NOG mouse reconstituted with CB-derived $CD34^+$ cells; DNP-KLH = 2,4-dinitrophenol-conjugated keyhole-limpet-hemocyanin; EBV = Epstein-Barr virus; H = exHer-2; Ig = immunoglobulin; ND = not determined; P/S = peptide and SV22; S = SV22.
Antibody production was determined by enzyme-linked immunosorbent assay for culture supernatants. Four clones were exHer-2–specific. Forty-eight clones were epitope peptide-specific. One of the clones stably produced antibodies for more than 7 months.
[a]Mouse pooled for one fusion experiment.
[b]Total cell number used for one fusion experiment.

not so different between the peptide-immunized and nonimmunized groups. These results indicate that immunization of a certain peptide derived from the membrane protein can induce specific antibodies in CB-NOG mice, but that its antigenicity is not as strong as the whole molecule including the epitope sequence expressed on the cell surface.

Only IgM was detectable as antigen-specific antibodies in the sera of CB-NOG mice when mice were immunized with either peptide or ordinary protein antigens. In consideration of the characters of CB-NOG mice, this result might not be unexpected: the majority of spleen B cells of CB-NOG are $CD5^+B1$ cells [12], which are recognized as being the major IgM producer. However, human B cells developed in CB-NOG mice have a potential to produce IgG, because nonspecific IgG was detected in the CB-NOG mice immunized with Her-2 peptide. Very recently, Ishiawa et al. [25] reported development of specific IgG against ovalbumin in newborn NOG mice receiving transplantation of human stem cells, although the antibody level was not high enough. Therefore, it is possible that the cognate interaction mediated by a certain antigen on major histocompatibility class (MHC) II between B cells and T cells may occur in a low frequency, presumably because most human T cells developed in the mouse thymus of CB-NOG mice are restricted with mouse MHC. Consequently, only a low proportion of B cells can recognize helper T cells by human MHC restriction to secrete antigen-specific IgG (in preparation).

To date, most human monoclonal antibodies were prepared from mouse–human hybridoma lines prepared by human B cells and mouse myeloma cell lines, mainly because the adequate human myeloma cell line was not available. Recently, Karpas and his collaborators established a myeloma cell line, Karpas707H, which expresses a low level of human light chain without its secretion. Using this myeloma cell line, they succeeded in establishing genuine

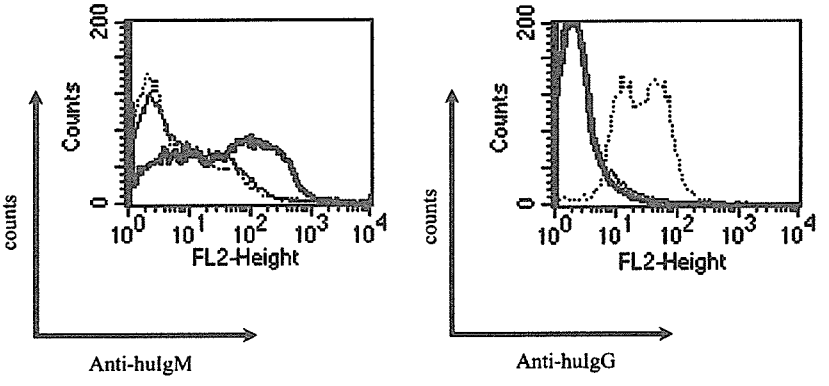

Figure 3. Recognition of surface Her-2 by human anti-Her-2 immunoglobulin M (IgM). Anti-Her-2 IgM was prepared from human hybridoma and purified. Mouse B-cell lymphoma (A20) expressing Her-2 was stained with the anti-peptide IgM antibody prepared from one of the hybridoma lines or Herceptin (IgG). Phycoerythrin-conjugated anti-human IgM (Anti-huIgM) or anti-human IgG (Anti-huIgG) was used for the secondary antibody. Cells were washed and analyzed by fluorescein-activated cell sorting analysis. Bold lines show the staining pattern with anti-peptide IgM; dotted lines show that of Herceptin. Solid thin lines show that of only secondary antibody.

human hybridomas by fusing with EBV transformed human B cell line producing anti-HIV-1 IgG and with fresh cells obtained from tonsils or peripheral blood cells. According to their process, we fused Karpas707H with spleen cells obtained from CB-NOG mice immunized with given antigens. Corresponding to the spectrum of the immunoglobulin type in the serum of the immunized CB-NOG mice, all the hybridomas we established secreted IgM antibody against Her-2 peptide (Table 4). Among these, one of the hybridoma lines maintained production of anti-Her-2 peptide antibody in the culture for more than 7 months without losing IgM secretion ability, and the partially purified antibody recognized Her-2 transfectants. Corresponding to the serum Igs, some of the hybridoma lines were found to secrete nonspecific IgG antibodies, indicating that at least EBV transformation of B cells in vitro does not disturb the fusion of Karpas707H with spleen B cells producing either IgG or IgM in CB-NOG.

IgG-type monoclonal antibody is considered more useful for clinical usage mainly because of its low molecular weight, high specificity, and multifunctions. However, IgM may not always be invalid for clinical application. For example, IgM antibodies against HIV induce more efficient cytolysis for infected cells in a complement-mediated manner presumably because the complement binding ability of IgM is higher than IgG [26]. Although our monoclonal IgM antibody showed very low cytotoxic activity against Her-2–positive tumor in vitro under the presence of mouse serum (data not shown), several groups reported that IgM antibodies possess anti-tumor function in the presence of complements [27–31]. Thus, the method described in this article will be useful in obtaining genuine human monoclonal antibody to the surface molecule on tumor cells, even if the antibody is IgM.

In summary, we demonstrated that CB-NOG mice, which were prepared from immunodeficient NOG mice reconstituted with human immune system, have potential for producing peptide-antigen–specific IgM antibodies, although most B cells developed in the mice are $CD5^+$ cells. We could produce human-derived IgM antibody against Her-2 epitope peptide in the CB-NOG mice. By fusing splenic B cells from the immunized NOG mice with a human myeloma cell line, we succeeded to generate genuine human hybridoma secreting antigen-specific IgM against a given peptide.

References

1. Osbourn J, Jermutus L, Duncan A. Current methods for the generation of human antibodies for the treatment of autoimmune diseases. Drug Discov Today. 2003;8:845–851.
2. Stern M, Herrmann R. Overview of monoclonal antibodies in cancer therapy: present and promise. Crit Rev Oncol/Hematol. 2005;54:11–29.
3. Glennie M, van de Winkel J. Renaissance of cancer therapeutic antibodies. Drug Discov Today. 2003;8:503–510.
4. Hochberg M, Lebwohl M, Plevy S, Hobbs K, Yocum D. The benefit/-risk profile of TNF-blocking agents: findings of a consensus panel. Semin Arthritis Rheum. 2005;34:819–836.
5. Botsios C. Safety of tumour necrosis factor and interleukin-1 blocking agents in rheumatic diseases. Autoimmun Rev. 2005;4:162–170.
6. Qu Z, Griffiths G, Wegener W, et al. Development of humanized antibodies as cancer therapeutics. Methods. 2005;36:84–95.
7. Tomizuka K, Shinohara T, Yoshieda H, et al. Double trans-chromosomic mice: maintenance of two individual human chromosome fragments containing Ig heavy and k loci and expression of fully human antibodies. Proc Natl Acad Sci U S A. 2000;97:722–727.
8. Mirick G, Bradt B, Denardo S, Denardo G. A review of human anti-globulin antibody (HAGA, HAMA, HACA, HAHA) responses to monoclonal anitbodies. Not four letter words. Q J Nucl Med Mol Imaging. 2004;48:251–257.
9. Li C, Ando K, Kametani Y, et al. Reconstitution of functional human B lymphocytes in NOD/SCID mice engrafted with ex vivo expanded CD34(+) cord blood cells. Exp Hematol. 2002;30:1036–1043.
10. Saito Y, Kametani Y, Hozumi K, et al. The in vivo development of human T cells from CD34(+) cells in the murine thymic environment. Int Immunol. 2002;14:1113–1124.
11. Ito M, Hiramatsu H, Kobayashi K, et al. NOD/SCID/gamma(c)(null) mouse: an excellent recipient mouse model for engagement of human cells. Blood. 2002;100:3175–3182.
12. Matumura T, Kametani Y, Ando K, et al. Functional CD5+ B cells develop predominantly in the spleen of NOD/SCID/gc^{null} (NOG) mice transplanted either with human umbilical cord blood, bone marrow, or mobilized peripheral blood CD34+ cells. Exp Hematol. 2003;31:789–797.
13. Lucchese A, Stevanovic S, Sinha A, Mitterlman A, Kanduc D. role of MHC II affinity and molecular mimicry in defining anti-HER-2/neu MAb-3 linear peptide epitope. Peptides. 2003;24:193–197.
14. Klapper L, Vaisman N, Hurwitz E, et al. A subclass of tumor-inhibitory monoclonal antibodies to ErbB-2/HER2 blocks crosstalk with growth factor receptors. Oncogene. 1997;14:2099–2109.
15. Shawver L, Mann E, Elliger S, Dugger E, Arteaga C. Ligand-like effects induced by anti-c-erbB-2 antibodies do not correlate with and are not required for growth inhibition of human carcinoma cells. Cancer Res. 1994;54:1367–1373.
16. Yip Y, Smith G, Koch J, Dubel S, Ward RL. Identification of epitope regions recognized by tumor inhibitory and stimulatory anti-ErbB-2 monoclonal anitbodies: implications for vaccine design. J Immunol. 2001;166:5271–5278.
17. Ishida T, Tsujisaki M, Hinoda Y, Imai K, Yachi A. Establishment and characterization of mouse-human chimeric monoclonal anitbody to *erbB-2* product. Jpn J Cancer Res. 1994;85:172–178.
18. Karpas A, Dremucheva A, Czepulkowski B. A human myeloma cell line suitable for the generation of human monoclonal antibodies. Proc Natl Acad Sci U S A. 2001;98:1799–1804.
19. Ishida T, Tsujisaki M, Hanzawa Y, et al. Significance of erbB-2 gene product as a target molecule for cancer therapy. Scand J Immunol. 1994;39:459–466.
20. Tam J. Synthetic peptide vaccine design: synthesis and properties of a high-density multiple antigenic peptide system. Proc Natl Acad Sci U S A. 1988;85:5409–5413.
21. Basak A, Boudreault A, Chen A, et al. Application of the multiple antigenic peptides (MAP) strategy to the production of prohormone convertases antibodies: synthesis, characterization and use of 8-branched immunogenic peptides. J Pept Sci. 1995;1:385–395.
22. Beselga J, Tripathy D, Mendelsohn J, et al. Phase II study of weekly intravenous Trastuzumab (Herceptin) in patients with Her2/neu-overexpressing metastatic breast cancer. Semin Oncol. 1999;26:78–83.
23. Hiramatsu H, Nishikomori R, Heike T, et al. Complete reconstitution of human lymphocytes from cord blood CD34+ cells using the NOD/SCID/gammacnull mice model. Blood. 2003;102:873–880.

Lentivirus vectors expressing short hairpin RNAs against the *U3*-overlapping region of HIV *nef* inhibit HIV replication and infectivity in primary macrophages

Takuya Yamamoto, Hiroyuki Miyoshi, Norio Yamamoto, Naoki Yamamoto, Jun-ichiro Inoue, and Yasuko Tsunetsugu-Yokota

Although successful attempts to inhibit HIV-1 replication in T cells using RNAi have been reported, the effect of HIV-specific RNAi on macrophages is not well known. Macrophages are key targets for anti–HIV-1 therapy because they are able to survive long after the initial infection with HIV and can spread the virus to T cells. In this study, we identified a putative RNAi target of HIV, consisting of the portion of the *nef* gene overlapping the U3 region (Nef366), and generated a lentivirus-based short hairpin RNA (shRNA) expression vector (Lenti shNef366). We show that Lenti shNef366 inhibits (1) HIV-1 replication in a monocytic cell line and in primary monocyte-derived macrophages (MDMs), (2) reactivation of latent HIV-1 infection, and (3) the production of secondary HIV-1 from MDMs harboring a genomic copy of Nef366. Moreover, we found that the up-regulated production of macrophage inflammatory protein 1β (MIP-1β), but not MIP-1α, in MDMs by Nef expression was considerably suppressed by Lenti shNef366, which suggests that HIV-1 dissemination to T cells through its interaction with HIV-1–infected MDMs can also be controlled by Lenti shNef366. Thus, lentivirus-mediated shRNA expression targeting the U3-overlapping region of HIV *nef* represents a feasible approach to genetic vaccine therapy for HIV-1. (Blood. 2006;108:3305-3312)

Introduction

HIV Nef, which is uniquely conserved among HIV-1, HIV-2, and SIV, is essential for viral replication in vivo.[1] Nef is located at the 3′ end of the viral genome, partially overlapping the 3′ long terminal repeat (LTR). The *nef* gene is one of the earliest expressed genes during HIV-1 replication and is transcribed at particularly high levels, often accounting for up to 80% of HIV-1–specific RNA in the early stages of viral replication. The Nef protein is multifunctional, having been shown to be involved in the down-regulation of CD4 receptor molecules, cell apoptosis, and signal transduction.[2-6] From studies of HIV-infected individuals, accumulating evidence indicates that Nef plays an important, albeit currently not clearly understood, role in the pathogenesis of AIDS.[1,2,6,7]

Recent investigations have shown that Nef has evolved macrophage-specific functions, such as the recruitment of T cells to sites of infection.[8] Macrophages expressing Nef secrete a high level of macrophage inflammatory protein 1α (MIP-1α) and MIP-1β, thus recruiting peripheral T cells to lymph nodes. More recently it was shown that Nef regulates the release of paracrine factors from macrophages[9]; at least 2 proteins have been identified, which enhance lymphocyte susceptibly to HIV-1 infection in the absence of cell-cycle progression. These results provide ample evidence that Nef functions as a virulence factor that contributes to the manifestation of the clinical symptoms of immunodeficiency. Thus, any therapeutic intervention aimed at either completely blocking or at least partially reducing the expression of *nef* during HIV infection would likely enhance the ability of the immune system to fight HIV infection.

Sequence-specific degradation of viral mRNA by the process of RNAi is a mechanism for selectively inhibiting the synthesis of viral proteins that are critical for HIV-1 replication. RNAi therapy is based on an existing mechanism of gene regulation that is ubiquitous in plants and animals, in which targeted mRNAs are degraded in a sequence-specific manner.[10] Quite recently, several groups reported the use of RNAi to successfully inhibit HIV-1 replication.[11-15]

To study the effect of stable expression of short hairpin RNA (shRNA) against the U3-overlapping region of HIV-1 *nef* on virus replication and Nef-mediated cytokine regulation in primary macrophages, we established a lentivirus vector system expressing HIV-specific shRNAs. We show that HIV replication in primary macrophages was considerably suppressed following transfection of shRNAs targeting the U3-overlapping region of genomic HIV *nef*. Moreover, RNAi was able to control CC-chemokine

From the Department of Immunology, National Institute of Infectious Diseases, Toyama, Shinjuku-ku, Tokyo; Subteam for Manipulation of Cell Fate, BioResource Center, RIKEN Tsukuba Institute, Tsukuba; Department of Molecular Virology, Bio-Response, Tokyo Medical and Dental University, Bunkyo-ku, Tokyo; AIDS Research Center, National Institute of Infectious Diseases, Shinjuku, Tokyo; and Division of Cellular and Molecular Biology, Department of Cancer Biology, Institute of Medical Science, University of Tokyo, Shirokane-dai, Minato-ku, Tokyo, Japan.

Submitted April 6, 2006; accepted June 29, 2006. Prepublished online as *Blood* First Edition Paper, July 20, 2006; DOI 10.1182/blood-2006-04-014829.

Supported by a grant from the Ministry of Health, Labor, and Welfare of Japan and from the Japan Health Sciences Foundation.

The authors declare no competing financial interests.

T.Y. and Y.T.-Y. performed laboratory experiments, data management, and the biostatistical analysis; T.Y., Naoki Y., J.-i.I., and Y.T.-Y. were responsible for the general design of the study; H.M. and Norio Y. were responsible for the design of the specific parts on lentivirus vectors and quantitative PCR analysis, respectively; T.Y., Y.T.-Y., and J.-i.I. were involved in the interpretation of the results and general outline of the paper; and T.Y. and Y.T.-Y. wrote the article.

Reprints: Yasuko Tsunetsugu-Yokota, Department of Immunology, National Institute of Infectious Diseases, Toyama 1-23-1, Shinjuku-ku, Tokyo 162-8640, Japan; e-mail: yyokota@nih.go.jp.

The publication costs of this article were defrayed in part by page charge payment. Therefore, and solely to indicate this fact, this article is hereby marked "advertisement" in accordance with 18 USC section 1734.

production associated with Nef expression in HIV-1–infected macrophages. Thus, lentivirus-vector–based RNAi of the *U3*-overlapping region of HIV-1 *nef* might have potential usefulness as a genetic vaccine against HIV-1 infection.

Materials and methods

Construction of plasmids

To express gene-specific shRNAs under the human U6-RNA promoter, sense and antisense oligonucleotides 47 bp in length were ligated into pENTR/U6 (Invitrogen, Carlsbad, CA). The sequences of the oligonucleotides were as follows: *lacz*, sense oligonucleotide, 5′-caccgctacacaaatcagcgatttcgaaaaatcgctgatttgtgtag-3′, and antisense oligonucleotide, 5′-aaaactacacaaatcagcgatttttcgaaatcgctgatttgtgtagc-3′; *Nef366* (nucleotides 366-385 of the HIV-1_{NL432} *nef* ORF overlapping the 3′ LTR), sense oligonucleotide, 5′-caccgattggcagaactacacaccaagagagtgtgtagttctgccaatc-3′, and antisense oligonucleotide, 5′-aaaagattggcagaactacacactctct-tggtgtgtagttctgccaatc-3′. The resulting entry vectors were termed pENTR/shLacZ and pENTR/shNef366, respectively.

A Gateway-compatible (Invitrogen) HIV-1–based vector, pCS-RfA, containing elongation factor 1α promoter (EF-1α)–driven green fluorescent protein (EGFP) (pCS-RfA-EG),[16] was used to construct the lentivirus vectors, pCS-EG/shLacZ and pCS-EG/shNef366, according to the manufacturer's instructions (Invitrogen).

Cell culture and transfection

The human cell line 293T and human monocytic cell lines U937 and U1[17] were maintained in Dulbecco modified Eagle medium (DMEM) and RPMI 1640 medium (Gibco, Grand Island, NY), respectively, supplemented with 10% heat-inactivated fetal calf serum (FCS), penicillin (100 μg/mL), and streptomycin (100 μg/mL). To establish $CCR5^+$ CEMx174 cells expressing EGFP driven by HIV-LTR, CEMx174 cells were transfected with pEF-BOSbst-HuCCR5 and pHIV-1 LTR-EGFPpuro (kind gifts from M. Tatsumi, National Institute of Infectious Diseases, Tokyo, Japan) and CEMx174 CCR5/LTR-EGFP cells were established.

HeLa-CD4 cells (obtained from the National Institutes of Health AIDS Reagent Program) were transfected with pEF-Nef bst, and Nef-expressing HeLa-CD4 cells were established (HeLa-CD4-Nef).

RNAi target site selection

A Web-based program for designing siRNA targets (Promega, Madison, WI), BLOCK-iT RNAi Target Designer (Invitrogen), and the National Center for Biotechnology Information Web site were used for the selection of siRNA and shRNA sequences, and for BLAST searches. Stealth siRNAs were synthesized (Figure 1) and HeLa-CD4-Nef cells were transfected with 2.5 μL stealth siRNA complexed to 2.5 μL Lipofectamine 2000 (Invitrogen) according to the manufacturer's instructions. Total RNA was extracted and analyzed by quantitative reverse transcription–polymerase chain reaction (qRT-PCR) using specific LUX primers (Invitrogen) and the SuperScript III Platinum One-Step Quantitative RT-PCR system (Invitrogen). The sequences of the qRT-PCR primers were as follows: *nef* forward, labeled at its 3′ terminus with a reporter fluorophore 6-carboxyfluorescein (FAM), 5′-cagcagagtgtgattg-gatggcctgcFAMg-3′; *nef* reverse, 5′-tggctcagctcgtctcattctt-3′; *ef-1α* forward labeled at its 3′ terminus with a reporter fluorophore 6-carboxy-4′, 5′-dichloro-2′, 7′-dimethoxyfluorescein (JOE), 5′-gaaccacaagtgctaa-catgccttggJOEtc-3′; *ef-1α* reverse, 5′-agcgtggttccactggcatt-3′. The reactions were performed using an Mx3000P (Stratagene, La Jolla, CA).

For Western blot analysis, cell lysates were prepared, subjected to 12.5% sodium dodecyl sulfate–polyacrylamide gel electrophoresis (SDS-PAGE), and immunoblotted with anti-Nef monoclonal antibody (mAb; F3, a kind gift from Dr Y. Fuji, Graduate School of Pharmaceutical Science, Nagoya City University, Nagoya, Japan). The blot was reacted with biotinylated goat anti–mouse IgG antibody (Jackson ImmunoResearch, West Grove, PA), then with streptavidin-POD (Roche, Indianapolis, IN).

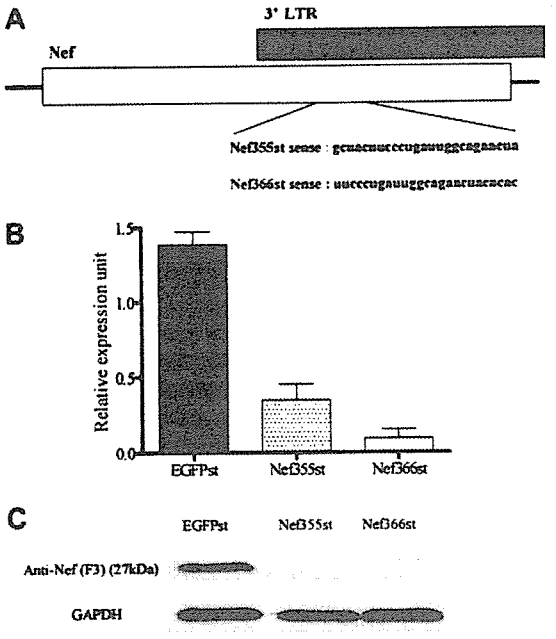

Figure 1. siRNA target sequences in *nef*. (A) Targets of siRNAs against the U3-overlapping region of HIV-1_{NL432} Nef and their sequences. Nef-expressing HeLa CD4 cells were transfected either with 2.5 μM *egfp* siRNAs (control: EGFPst) or *nef* siRNAs (Nef355st or Nef366st). At 48 hours after transfection, these cells were lysed to obtain total RNA and protein. (B) Total RNA was extracted and analyzed by qRT-PCR. The level of *nef* mRNA expression was normalized with that of elongation factor 1α (EF-1α) mRNA expression (*nef*/EF-1α). The data represent the expression level of *nef* mRNA relative to that of the control as 100%. The data represent the average ± SD of 3 independent experiments. (C) The cell lysates were subjected to 12.5% SDS-PAGE and immunoblotted with anti-Nef mAb.

Proteins were visualized by the SuperSignal Western Dura Extended Duration Substrate (Pierce, Rockford, IL) using an LAS3000 analyzer (Fuji Film, Tokyo, Japan).

Preparation of lentivirus vector

The lentivirus shRNA expression vectors were produced by transient transfection of 293T cells with a self-inactivating (SIN) vector construct, VSV-G– and Rev-expressing plasmid pCMV-VSV-G-RSV-Rev, and the packaging construct pCAG-HIVgp using the calcium phosphate precipitation method.[16] The lentiviral vector was concentrated by ultracentrifugation and the final solution was assayed for p24 antigen by an in-house enzyme-linked immunosorbent assay (ELISA).[18] The infectivity was determined by using 293T cells based on the EGFP expression.

Preparation of HIV-1 virus stocks

To prepare HIV-1, COS-7 cells were transfected with either pNL432, pNF462 (a kind gift from A. Adachi, Tokushima University, Tokushima, Japan), or pNF462dNef, in which the *nef* gene was deleted by digestion with *Xho*I and *Kpn*I, as described previously.[18]

Primary MDM culture

From peripheral blood mononuclear cells (PBMCs) of healthy, $HIV\text{-}1^-$ donors, $CD14^+$ monocytes were enriched using a magnetic-activated cell sorter (MACS; Miltenyi Biotec, Cologne, Germany) as described.[18] Monocytes were cultivated in RPMI 1640 medium supplemented with 10% FCS, 5% human AB plasma, and 10 ng/mL macrophage colony-stimulating factor (M-CSF) for 1 week to allow differentiation into monocyte-derived macrophages (MDMs).

Kinetics of virus production in stable shRNA-expressing U937 cells

Stable shRNA-expressing cells were infected with HIV-1_{NL432} for 2 hours, then cells were washed 5 times. Culture supernatants were harvested at 3- or

4-day intervals and viral production was monitored by HIV of p24 Gag antigen ELISA kit (RETRO TEC; ZeptoMetrix, Buffalo, NY).

Real-time RT-PCR (qRT-PCR) analysis of HIV-1 infection

HIV-1–infected cells were collected and total DNA was prepared 3, 8 and 12 hours after infection. For the detection and quantification of individual forms of HIV-1 DNA, oligonucleotide primer and probe sequences were designed specifically for the *Taq*Man assay as described elsewhere.[19] All probes (Biosearch Technologies, Novato, CA.) were 5′-labeled with the fluorophore FAM as the reporter dye, and 3′-labeled with Black Hole Quencher-1 (BHQ-1) as the quencher dye. The qRT-PCR analysis was performed on an Mx3000P (Stratagene) and the amount of HIV-1–specific DNA per cell was normalized to β-globin gene.

Kinetics of virus production in MDMs and reporter analysis

MDMs (2×10^5/well) were cultured in 48-well tissue-culture plates and infected either with wild-type HIV-1_{NF462} or HIV-$1_{NF462\Delta Nef}$. MDMs were infected with lentivirus at a multiplicity of infection (MOI) of 2 or 10 and washed extensively. The next day, cells were exposed to HIV-1 (5 ng/well) for 2 hours. Cell supernatants were harvested at 3- or 4-day intervals, and viral production was monitored by p24 antigen ELISA.

The cell-culture supernatants at 10 days after HIV infection were examined for infectivity, and 10 days after HIV infection, cell supernatants were collected (termed HIV-1/Lenti cont and HIV-1/Lenti shNef366). CEMx174 CCR5/LTR-EGFP cells were infected with HIV-1/Lenti cont or HIV-1/Lenti shNef366, and the number of HIV-1–infected $EGFP^+$ T cells was determined by fluorescence-activated cell sorter (FACS).

Detection of chemokines

For the detection of chemokine production in MDMs, the cytometric bead array (CBA) kit (BD Bioscience, San Jose, CA) was used, which measured 4 chemokines (IL-8, MIP-1α, MIP-1β, MCP-1) simultaneously.

Restimulation assay of lentivirus-transduced U1 cells

Latent HIV-1–infected U1 cells were transduced with Lenti cont or Lenti shNef366 at an MOI of 1. Two weeks later, $EGFP^+$ cells were sorted and stimulated with 1 ng/mL recombinant granulocyte-macrophage colony-stimulating factor (GM-CSF). Culture supernatants were collected at days 2 and 5, and the level of p24 antigen was measured by ELISA.

Results

siRNA suppresses *nef* mRNA and Nef protein expression

In the HIV-1 genome, *nef* is located at the 3′ end of the viral genome, partially overlapping the 3′ LTR (Figure 1A). Jacque and colleagues demonstrated previously that siRNA targeting of the 5′ region of *nef* (nucleotides 164-185) suppressed HIV replication.[20] Therefore, we selected 3 distinct regions of the HIV-1_{NL432} *nef* sequence using a Web-based program for designing DNA-directed RNAi systems, focusing on the Nef coding region overlapping the 3′ LTR. These were designated as Nef338, 366, and 479 based on the position of the first nucleotide of the siRNA. From initial screening experiments, we found that Nef366 was the most effective target site (data not shown).

The type 1 interferon response is an innate defense mechanism in eukaryote cells against viral infection. It has been shown that some types of siRNA induce type 1 interferon, which in turn mediates the gene-specific effect of RNAi.[21-23] The stealth siRNA system was developed to avoid the interferon response to siRNA in cells (Invitrogen manual). We prepared synthetic stealth siRNAs, designated Nef355st and Nef366st, and a control siRNA designated EGFPst, to determine the effect of RNAi using sequences based on Nef366 (the U3-overlapping region of the Nef-coding region). Neff355st was synthesized based on a Web-based computer program for generating stealth siRNA (Invitrogen), whereas Nef366st represents a slightly modified version of the stealth target site (6-nucleotide difference), so that it conformed to the target sequence as described. These stealth Nef siRNA sequences differed by only 5 nucleotides (Figure 1A).

We established a stable Nef-expressing HeLa-CD4 clonal cell line, designated as HeLa-CD4-Nef. HeLa-CD4-Nef cells were transfected either with 2.5 μM EGFPst or *nef* stealth siRNAs (Nef355st or Nef366st), and harvested 48 hours after transfection. Total RNA was extracted and the level of *nef* mRNA was measured by qRT-PCR. We observed that transfection with Nef366st reduced *nef* mRNA expression more than 90% (Figure 1B), whereas Nef355st suppressed the level of *nef* mRNA approximately 80%, compared with EGFPst controls. When cell lysates of the transfected cells were analyzed by Western blot, we found that both Nef366st and Nef355st suppressed Nef protein levels to below the detection limit of the assay (Figure 1C). Taken together, these results clearly showed that Nef366 is an efficient target sequence for the inhibition of *nef* gene expression by siRNA.

shRNA suppresses *nef* mRNA and Nef protein expression

To assess the effect of endogenous expression of Nef366 siRNA, we constructed expression vectors that encoded shRNAs corresponding to Nef366, or *lacZ* as a control, driven by the human U6 polymerase III promoter, designated as pENTR/shNef366 and pENTR/shLacZ, respectively (Figure 2A). HeLa-CD4-Nef cells were transfected with either pENTR/shNef366 or pENTR/shLacZ by FuGene6 reagent (Roche) and cells were harvested 72 hours after transfection. Total RNA was extracted and analyzed by qRT-PCR. We observed that the level of *nef* mRNA was suppressed by approximately 80% in cells transfected with pENTR/shNef366 (Figure 2B). Western blot analysis confirmed that pENTR/shNef366 strongly suppressed Nef protein levels as well (data not shown). These results indicated that promoter-driven endogenous

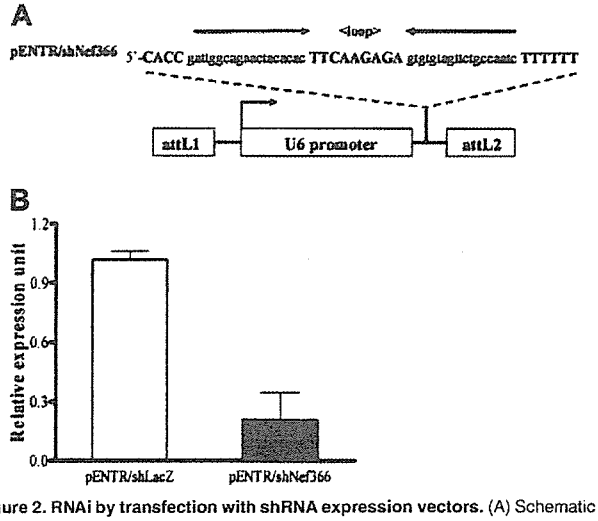

Figure 2. RNAi by transfection with shRNA expression vectors. (A) Schematic of the expression vectors (pENTR/shRNA) encoding shRNAs of Nef366 or *lacZ*, designated as pENTR/shNef366 and pENTR/shLacZ, respectively, in which expression is driven by the human U6 polymerase III promoter. (B) Nef-expressing HeLa-CD4 cells were transfected either with 1.0 μg pENTR/shNef366 or pENTR/shLacZ and cells were harvested 72 hours after transfection. Total RNA was extracted and analyzed by qRT-PCR. The data represent the average ± SD of 3 independent experiments.

expression of shNef366 was able to mediate RNAi of *nef* in HeLa-CD4-Nef cells.

Inhibition of HIV-1 replication in U937 cells by lentivirus-based shRNA expression

The transfection efficiency of the entry vectors used in suspension cells was quite low, and the objective here is to introduce siRNAs into primary macrophages. Therefore we constructed HIV-1–based lentivirus vectors expressing Nef366 shRNA or shRNA targeting lacZ as a control (Lenti shNef366 and Lenti control) using Gateway technology. The structure of the lentivirus vector used in the following studies is illustrated in Figure 3A.

To test whether Nef366 shRNA was able to efficiently block HIV-1 replication, we infected U937 cells with Lenti shNef366 or Lenti control, both of which encoded GFP driven by the EF-1α promoter (EGFP), at an MOI of 1. Two weeks after infection, nearly 30% of the cells stably expressed EGFP (Figure 3B upper panel). We sorted the EGFP$^+$ cells by fluorescence-activated cell sorter (FACSaria; BD Biosciences), after which the purity of the Lenti control– and Lenti shNef366–transfected, EGFP$^+$ cells was 97.2% and 99.7%, respectively (Figure 3B lower panel; U937/Lenti cont and U937/Lenti shNef366). The purified cell populations were then infected with 2 inoculation doses of HIV-1 (Figure 3C upper and lower panels; p24: 20 ng and 100 ng, respectively). The culture supernatants were collected at 3- or 4-day intervals, and the level of p24 antigen was measured by ELISA. We observed that at both inoculation doses HIV-1 replication in U937 cells was inhibited by Lenti shNef366, especially at the peak of HIV-1 production. The reverse transcriptase activity was also measured in parallel, and the result was consistent with that of p24 ELISA (data not shown). The inhibition of HIV-1 replication was sustained at least for 1 week, following which HIV-1 production gradually decreased in all cell populations, presumably because of the cytopathic effect of HIV-1 infection.

To further evaluate the effect of RNAi on the early steps of HIV-1 infection, we prepared cell lysates at different time points after inoculation (3, 8, and 12 hours after infection) and analyzed the level of reverse transcription activity by measuring the amount of different forms of proviral DNA (HIV-1 *2LTR* and *U5-Gag*) by the qRT-PCR. The copy number of these proviral DNA forms decreased in U937/Lenti shNef366 cells, relative to that seen in U937/Lenti control cells at all time points. The amount of these DNA forms normalized to β-globin gene at 12 hours after HIV-1 infection is depicted in Figure 3D. The copy number of *2LTR* and *U5-Gag* was 16.9% and 13.4% of control, respectively. These results suggested that the inhibition of HIV-1 replication occurred early after virus entry, presumably during uncoating or reverse transcription, not integration.

A type 1 interferon response has been shown to be induced by synthetic siRNAs via protein kinase R- (PKR) or toll-like receptor 7 (TLR 7)–mediated signaling pathways.[21-23] To eliminate the possibility that we were generating an interferon response following shRNA expression in our system, we analyzed the level of 2′ 5′-oligoadenylate synthetase mRNA expression in Lenti shNef366–infected U937 cells by qRT-PCR. We detected no such message (data not shown), indicating that the interferon response plays a

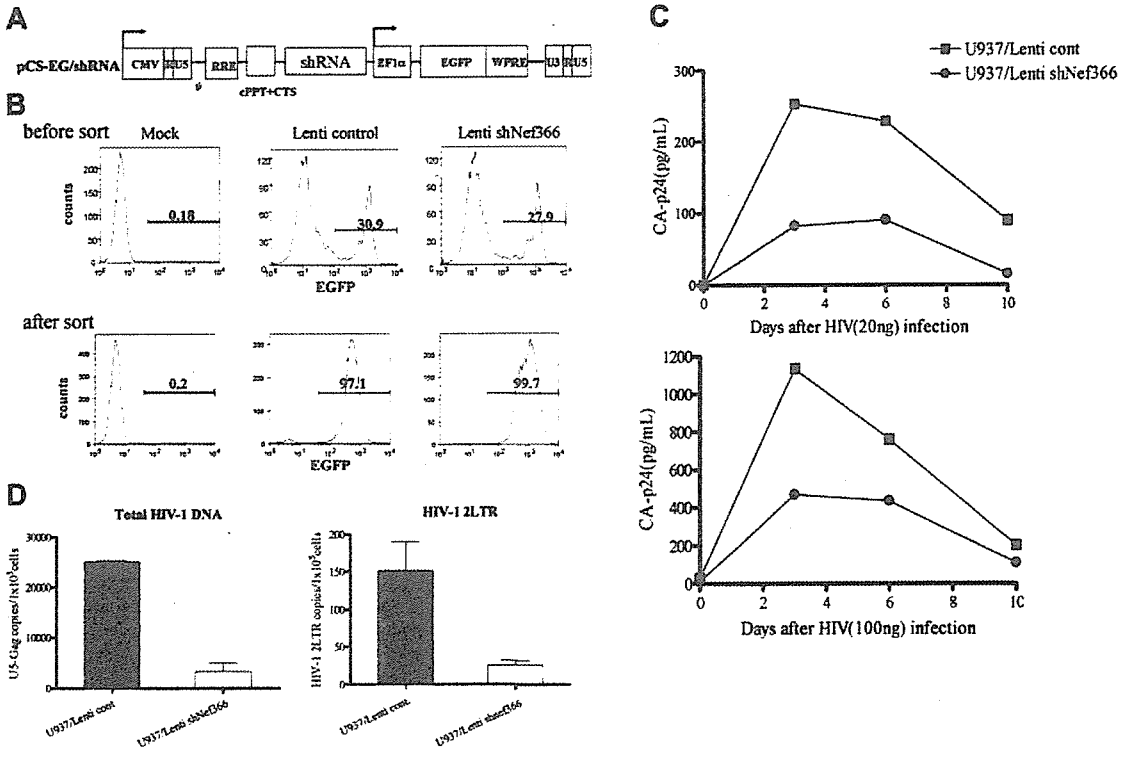

Figure 3. Inhibition of HIV-1 replication in U937 cells by lentivirus-mediated shRNA. (A) The structure of the shRNA lentiviral expression vector. The HIV-1–based lentivirus vector for expressing shRNA was constructed using Gateway technology. pCS-EG/shRNA consisted of U6-shRNA upstream of an EF1α promoter–driven EGFP expression cassette, which allowed simultaneous expression of shRNA and EGFP. (B) U937 cells were infected with lentivirus expressing either shNef366 (Lenti shNef366) or shLacZ (Lenti control) at an MOI of 1. After 2 hours of infection, cells were washed and maintained in culture. Cells expressing EGFP were analyzed by FACS, and EGFP$^+$ cells were collected. EGFP$^+$ cells were analyzed by FACSaria 1 week later (designated as U937/Lenti control and U937/Lenti shNef366). (C) U937/Lenti cont or U937/Lenti shNef366 cells (1×10^5/well) were infected with HIV-1_{NL432}, and the culture supernatants of these cells were collected at 3- or 4-day intervals after infection. The level of p24 antigen in the culture supernatants was measured by ELISA. (D) HIV-1–infected cells were collected and total DNA was prepared 12 hours after infection. Total HIV-1 and 2LTR DNA was analyzed by qRT-PCR. The amount of HIV-1–specific DNA per cell was normalized to β-globin gene expression. The data represent the average ± SD of 3 independent experiments.

minimal role, if any, in the observed inhibitory effect on HIV replication by Lenti shNef366.

Lentivirus-based nef shRNA inhibits HIV-1 replication and affects chemokine production in MDMs

Swingler and coworkers reported that HIV-1 Nef expression in macrophages mediated lymphocyte chemotaxis and activation through the induction of MIP-1α and MIP-1β expresion.[8] To determine the effect of Nef expression during HIV-1 infection in MDMs, we infected MDMs with wild-type HIV-1_{NF462} or the corresponding *nef* gene-deletion mutant, HIV-1_{NF462}dNef, and assessed the kinetics of virus replication by p24-specific ELISA. Representative results from 2 donors are shown in Figure 4A. We consistently observed that the level of HIV-1_{NF462} replication was 2- to 6-fold higher than that of HIV-1_{NF462}dNef in MDMs. These results were consistent with those reported by Swingler et al.[9] Although no apparent T-cell damage was observed during cultivation for 3 weeks following HIV-1 infection, the amount of virus production gradually decreased. We analyzed chemokine production in MDMs infected with HIV-1 wild-type and *nef*-deleted HIV-1 at days 10, 14, and 17 after infection. The level of chemokine production in uninfected MDMs varied depending on the donor, but both donors produced a high level of IL-8 and monocyte chemotactic protein-1 (MCP-1), and a low level of MIP-1α and MIP-1β (data not shown). HIV infection per se, independent of the presence or absence of Nef, did not affect this trend, in that the levels of these chemokines, with the exception of MIP-1β, were only slightly affected by HIV infection. Notably, virus replication resulted in an increased production of MIP-1β, which peaked at 14 days after infection, in parallel with the peak of viral replication. Figure 4B shows the results of the analysis of the levels of MIP-1β and MIP-1α in the 2 donors. HIV-1 infection induced a 2-fold increase in the level of MIP-1β compared with mock-infected MDMs. In contrast, infection with Nef-deleted HIV-1 caused a reduction in the level of MIP-1β in the MDMs from both donors, indicating that Nef is responsible for the up-regulation of MIP-1β, but does not affect MIP-1α, MCP-1, or IL-8 production.

To examine whether shRNAs against the U3-overlapping region of *nef* were able to block HIV-1 replication in MDMs, we infected MDMs with Lenti control or Lenti shNef366, at an MOI of 10 or 2 (Figure 5A left and right panels, respectively). After 2 hours of incubation, cells were extensively washed and cultivated overnight, and the following day, they were infected with HIV-1_{NF462}. Culture supernatants were collected every 3 or 4 days and the level of p24 antigen was measured by ELISA. Of note, despite the extensive washing after lentivirus infection, the level of p24 was quite high up to 7 days after HIV-1 infection. We detected a second peak of virus production, which we interpreted as true HIV-1 replication in MDMs transduced with lentiviral vectors expressing shRNAs. In addition, presumably because of the toxic effect of infection by lentivirus pseudotyped with VSV, the level of p24 antigen was lower than that in MDMs infected with HIV-1 virus. Nevertheless, we observed a similar level of inhibition of HIV-1 replication in MDMs by Lenti shNef366 at 2 different doses of infection (Figure 5A), and the inhibition was maintained for at least 3 weeks after HIV-1 infection.

Macrophages can mediate efficient infection of lymphocytes *in trans*,[9,24] suggesting that macrophages serve as a major reservoir and vehicle for HIV-1 dissemination. We were interested in whether the progeny virus produced from MDMs harboring Nef366 shRNA maintained their ability to infect T cells. Supernatants from MDM cells transduced with Lenti control or Lenti shNef366 were collected 10 days after HIV infection, and the level of p24 antigen was measured and used to quantitate the amount of HIV present. These sources of HIV were designated as HIV/Lenti cont or HIV/Lenti shNef366. Using CEMx174 CCR5/LTR-EGFP cells as indicator cells, we estimated the infectivity of HIV/Lenti cont or HIV/Lenti shNef366 by analyzing the number of $EGFP^+$ T cells following infection (Figure 5B). Compared with HIV-1/Lenti cont, HIV-1/Lenti shNef366 had a significant loss of infectivity in $CCR5^+$ T cells. Our results suggested that Lenti shNef366 has the potential to protect HIV-1 dissemination to T cells by HIV-1–infected MDMs

We also examined the level of chemokine production following HIV infection of MDMs transduced with shRNA lentivirus vectors. Although the basal level of MIP-1α and MIP-1β production was slightly increased following lentivirus infection, the level of MIP-1β decreased in Lenti shNef366 cells compared with Lenti control (Figure 5C). The levels of MCP-1 and IL-8 were either unaffected or somewhat restored by Lenti shNef366 (data not shown).

Lentivirus-based nef shRNA protects progression from latent HIV-1 infection to productive infection

Latent HIV-1 infection can be established following provirus integration into the host genome.[25-27] A small number of infected cells re-enter the resting stage, harboring an integrated copy of the HIV-1 genome. These latent HIV-infected cells represent a barrier to successful virus eradication because subsequent cytokine or

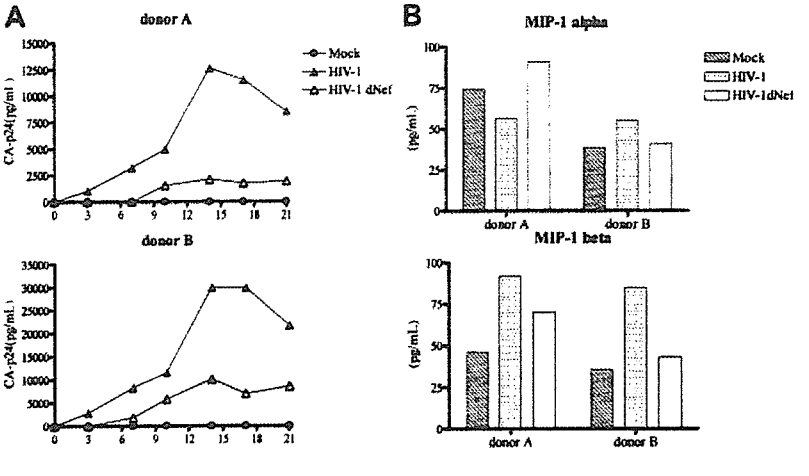

Figure 4. The effect of Nef expression during HIV-1 infection in MDMs. (A) MDMs (2×10^5/well) of 2 donors were infected either with wild-type HIV-1_{NF462} or HIV-$1_{NF462dNef}$. The supernatants of these wells were harvested at 3- or 4-day intervals after infection, and viral production was monitored by sequential quantitation of p24 by ELISA. (B) The CBA kit was used to measure the level of chemokines (MIP-1α and MIP-1β) in cell supernatants 14 days after HIV infection.

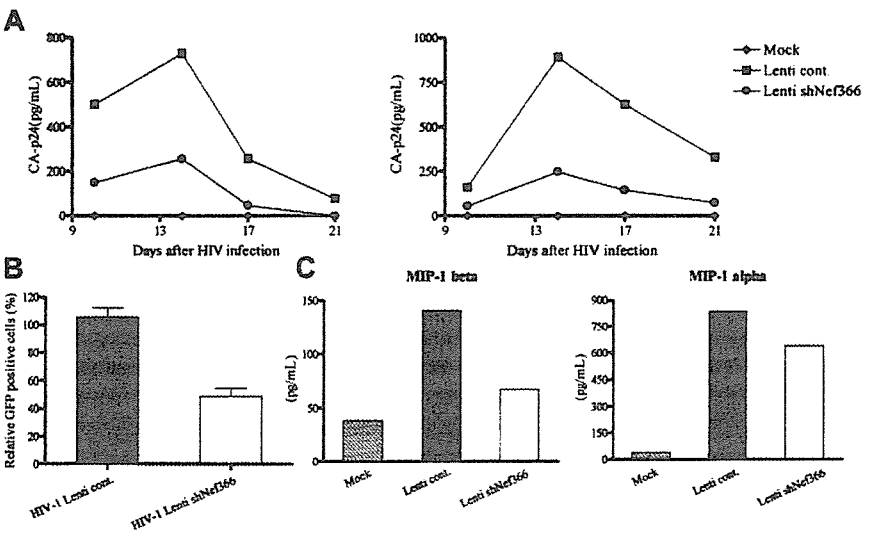

Figure 5. Lentivirus-expressed nef shRNA inhibits HIV-1 replication and affects chemokine production in MDMs. (A) MDMs were transduced with Lenti cont or Lenti shNef366 at an MOI of 2. At 2 hours after infection, cells were washed twice, then cultured for another 24 hours, at which point the cells were infected with HIV-1_{NF462}. The culture supernatants were collected at 3- or 4-day intervals after HIV infection, and the level of p24 antigen was measured by ELISA. (B) MDMs transduced either with Lenti control or Lenti shNef366 were infected with HIV-1 and supernatants were collected 10 days after infection and designated as HIV-1 Lenti cont and HIV-1 Lenti shNef366, respectively, CEMx174 CCR5/LTR-EGFP cells were infected either with HIV-1 Lenti cont or HIV-1 Lenti shNef366 and GFP^+, HIV-1–infected T cells were analyzed by FACS 48 hours later. The data represent the average ± SD of 3 independent experiments. (C) The culture supernatants of MDMs transduced with lentivirus vectors were collected 14 days after infection and the levels of the chemokines MIP-1α and MIP-1β were measured.

other stimuli can reactivate viral gene expression, and reinitiate HIV-1 replication.[28-31] We were interested in whether Lenti shNef366 was able to regulate the progression of latent HIV-1 infection to productive infection in U1 cells.[17] U1 cells are U937 cells in which a latent HIV-infection has been established, and HIV-1 replication can be induced in these cells on appropriate activation. We transduced U1 cells with Lenti control or Lenti shNef366 at an MOI of 1. After 2 hours of infection, cells were extensively washed and maintained in culture. Two weeks after transduction, the cells were sorted by FACSaria, and the $EGFP^+$ cell population was stimulated with 1 ng/mL recombinant GM-CSF. Culture supernatants were collected at different time points (days 2 and 5) and the level of p24 antigen was measured by ELISA. As shown in Figure 6, the levels of p24 antigen were dramatically decreased in U1 cells harboring Lenti shNef366 at all time points examined.

Discussion

In this study, we constructed an shRNA expression system that targeted HIV *nef* gene sequences that overlap the 3′ LTR U3 (Nef366) and showed that Nef366 shRNA had a strong inhibitory effect on *nef* gene expression in Nef-expressing HeLa-CD4 cells. Furthermore, expression of shNef366 in monocytic cell lines strongly inhibited the replication of HIV-1 at an early stage of HIV infection. The rational for using shNef366 to target HIV *nef* was several-fold. Because the U3 region is required during reverse transcription for first template transfer and integration of the viral genome into the host genome, siRNA targeting of the U3 region may induce not only specific degradation of *nef* mRNA, but also inhibit HIV-1 reverse transcription. Furthermore, although others have observed escape mutations in RNAi experiments targeting *nef* or *tat*,[32,33] the nef/U3 sequence we targeted is highly conserved as discussed in the paragraph after the next one. If a mutation were to occur in the U3 region, it would affect the overall transcription efficiency of HIV-1 after integration because the U3 region of the HIV-1 LTR contains the transcription initiation or promoter/enhancer sites that are essential for efficient HIV transcription. Of note, the strategy used Jacque et al[20] using siRNA targeting of the 5′ region of *nef* turned out to induce an escape mutant.[33] Although we did not extensively test for the emergence of escape mutants, targeting the 3′ LTR U3-overlapping region of *nef* (Nef366) represented a potentially potent strategy for controlling HIV-1 replication.

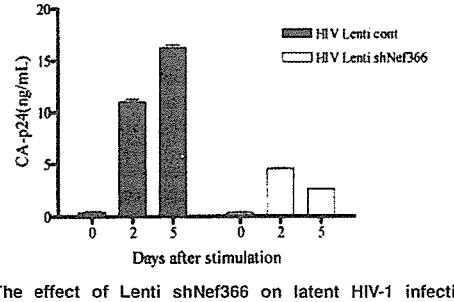

Figure 6. The effect of Lenti shNef366 on latent HIV-1 infection. Latent HIV-1–infected U1 cells were transduced with Lenti control or Lenti shNef366 at an MOI of 1. Two weeks after infection, $EGFP^+$ cells were sorted by FACSaria, and $EGFP^+$ cells were stimulated with 1 ng/mL recombinant GM-CSF. Cell-culture supernatants were collected 0, 2, and 5 days after stimulation, and the level of p24 antigen was measured by ELISA. The data represent the averages ± SDs of 3 independent experiments.

Macrophages are one of the major target cell populations in the early phase of HIV-1 infection, when R5 viruses predominate.[34] HIV-1 replication in macrophages is usually slow and less cytopathic compared with that in activated T cells, allowing the virus to survive long after infection. Thus, macrophages serve as one of the reservoirs for HIV in an infected individual.[35] Therefore, therapeutic strategies that target macrophages are promising approaches to the control of persistent HIV-1 infection in vivo. Taking advantage of the lentivirus expression system, which is an efficient way to introduce a desired gene into primary cells, we were able to show that expression of Nef366 shRNAs in primary MDMs inhibited HIV-1 replication in these cells.

In this context, several groups have demonstrated that RNAi, mediated by the introduction of HIV-specific siRNA duplexes, can inhibit viral replication in T cells, although the effect was transient.[20,36-38] Das et al were able to show a stable inhibitory effect on viral replication using a murine retrovirus vector expressing Nef-specific siRNAs in T-cell lines. However, the block in virus replication was not absolute and escape mutants emerged.[33] These previous results prompted us to develop a novel strategy of RNAi-mediated inhibition of HIV infection that did not induce a type 1 interferon and had a stable, long-term effect. We chose to

transduce Nef366 shRNA into low or nondividing primary macrophages, as opposed to actively proliferating T cells, using a lentivirus expression vector, and were able to demonstrate RNAi effect during macrophage cultivation for 3 weeks. Using an alignment of 200 HIV-1 sequences obtained by BLAST search analysis, only one base mismatch in the Nef366 region was detected in a subtype A virus (GenBank no. AB098332 and no. AB098333, HIV-1 UG029). Further study will be required to determine whether this subtype A virus is resistant to shRNA Nef366. Because Nef/LTR is in a completely conserved region, at least among subtype B viruses, this region might have quite an important function for HIV-1 replication. We speculate that if escape mutants were to emerge in the presence of lentiviral-shRNA Nef366, the compensatory mutation would occur outside of this region.

Importantly, using this system, we were also able to demonstrate a decrease in the infectivity of HIV-1 produced from infected MDMs. This attenuation effect is potentially significant because it implies that lentivirus-mediated RNAi may also reduce transmissibility of HIV-1 overall. However, in light of the significant problem of viral escape during chronic HIV infection, it may become necessary to combine multiple sites of siRNAs targeting the *nef-U3* region in the future.

Control of the latent phase of HIV infection is a key issue for effective therapeutic intervention. We demonstrated here that Lenti shNef366 was able to suppress the reactivation of HIV from latently infected cells. The expression of integrated HIV-1 in latently infected cells is controlled at the level of transcription by cellular factors and the viral transactivator Tat, both of which act through the HIV-1 LTR.[39] Transcription of integrated viral RNA is initiated at the R region of the 5′ LTR. The fact that shNef366, which targeted the U3-overlapping region of Nef, was effective in latently infected cells, suggests that shNef366 can directly target cleavage of *nef* mRNAs or total viral RNAs at the 3′ end. Therefore, our lentivirus-based shRNA expression system appears to be able to control both early and latent HIV-1 infection.

MIP-1α and MIP-1β are ligands of the HIV-1 coreceptor, CCR5. Through interaction with the CCR5 receptor, they promote the maturation of Th1 cells.[40,41] Swingler et al reported that MIP-1α and MIP-1β were induced by Nef in macrophages during HIV infection and that culture supernatants derived from Nef-expressing macrophages induced both chemotaxis and activation of resting T lymphocytes, enabling productive HIV-1 infection of those T cells.[8] These and other results have led to a model of HIV infection in which expression of Nef in HIV-infected MDMs enhances the secretion of MIP-1β, which recruits mainly $CCR5^+$ Th1 cells, resulting in the expansion of R5 tropic HIV-1 during macrophage–T-cell interactions. Our results were partially consistent with this model because the degradation of *nef* mRNA expression resulted in the decreased MIP-1β production. Of note, the production of MIP-1α in our system appeared to be unaffected by Nef expression but was induced by lentivirus infection. Because the production of MIP-1α in HIV-infected MDMs was similar to that in uninfected MDMs, it seems likely that MIP-1α production was enhanced by a non–HIV-specific component of the lentivirus expression system, perhaps VSV-G protein. Although the levels of MCP-1 and IL-8 varied depending on the donor and were independent of Nef expression, we cannot rule out the possibility that other unknown chemokines are induced by Nef. Any such dysregulated chemokine production by Nef expression in macrophages might provide an appropriate environment for HIV to establish an efficient infection and dissemination.

In summary, we demonstrated the feasibility of using lentiviral expression vectors to express shRNAs against the U3-overlapping region of *nef* in primary MDMs, as a type of intracellular immunization and potential gene therapy approach against HIV-1. Future development of an AIDS vaccine based on the specific inhibition of viral gene expression combined with existing therapeutic strategies may provide keys to help eradicate HIV.

Acknowledgments

We thank Masayuki Ishige and Rieko Iwaki for their excellent technical assistance.

References

1. Kestler HW 3rd, Ringler DJ, Mori K, et al. Importance of the nef gene for maintenance of high virus loads and for development of AIDS. Cell. 1991;65:651-662.
2. Agopian K, Wei BL, Garcia JV, Gabuzda D. A hydrophobic binding surface on the human immunodeficiency virus type 1 Nef core is critical for association with p21-activated kinase 2. J Virol. 2006;80:3050-3061.
3. Fackler OT, Baur AS. Live and let die: Nef functions beyond HIV replication. Immunity. 2002;16:493-497.
4. Geyer M, Fackler OT, Peterlin BM. Structure–function relationships in HIV-1 Nef. EMBO Rep. 2001;2:580-585.
5. Steffens CM, Hope TJ. Recent advances in the understanding of HIV accessory protein function. AIDS. 2001;15(suppl 5):S21-S26.
6. Na YS, Yoon K, Nam JG, et al. Nef from a primary isolate of human immunodeficiency virus type 1 lacking the EE(155) region shows decreased ability to down-regulate CD4. J Gen Virol. 2004;85:1451-1461.
7. Deacon NJ, Tsykin A, Solomon A, et al. Genomic structure of an attenuated quasi species of HIV-1 from a blood transfusion donor and recipients. Science. 1995;270:988-991.
8. Swingler S, Mann A, Jacque J, et al. HIV-1 Nef mediates lymphocyte chemotaxis and activation by infected macrophages. Nat Med. 1999;5:997-103.
9. Swingler S, Brichacek B, Jacque JM, Ulich C, Zhou J, Stevenson M. HIV-1 Nef intersects the macrophage CD40L signalling pathway to promote resting-cell infection. Nature. 2003;424:213-219.
10. Hannon GJ. RNA interference. Nature. 2002;418:244-251.
11. Coburn GA, Cullen BR. Potent and specific inhibition of human immunodeficiency virus type 1 replication by RNA interference. J Virol. 2002;76:9225-9231.
12. Lee MT, Coburn GA, McClure MO, Cullen BR. Inhibition of human immunodeficiency virus type 1 replication in primary macrophages by using Tat- or CCR5-specific small interfering RNAs expressed from a lentivirus vector. J Virol. 2003;77:11964-11972.
13. Novina CD, Murray MF, Dykxhoorn DM, et al. siRNA-directed inhibition of HIV-1 infection. Nat Med. 2002;8:681-686.
14. Qin XF, An DS, Chen IS, Baltimore D. Inhibiting HIV-1 infection in human T cells by lentiviral-mediated delivery of small interfering RNA against CCR5. Proc Natl Acad Sci U S A. 2003;100:183-188.
15. Song E, Lee SK, Dykxhoorn DM, et al. Sustained small interfering RNA-mediated human immunodeficiency virus type 1 inhibition in primary macrophages. J Virol. 2003;77:7174-7181.
16. Miyoshi H, Blomer U, Takahashi M, Gage FH, Verma IM. Development of a self-inactivating lentivirus vector. J Virol. 1998;72:8150-8157.
17. Folks TM, Justement J, Kinter A, Dinarello CA, Fauci AS. Cytokine-induced expression of HIV-1 in a chronically infected promonocyte cell line. Science. 1987;238:800-802.
18. Tsunetsugu-Yokota Y, Kato T, Yasuda S, et al. Transcriptional regulation of HIV-1 LTR during antigen-dependent activation of primary T cells by dendritic cells. J Leukoc Biol. 2000;67:432-440.
19. Yamamoto N, Tanaka C, Wu Y, et al. Analysis of human immunodeficiency virus type 1 integration by using a specific, sensitive and quantitative assay based on real-time polymerase chain reaction. Virus Genes. 2006;32:105-113.
20. Jacque JM, Triques K, Stevenson M. Modulation of HIV-1 replication by RNA interference. Nature. 2002;418:435-438.
21. Hornung V, Guenthner-Biller M, Bourquin C, et al. Sequence-specific potent induction of IFN-alpha by short interfering RNA in plasmacytoid dendritic cells through TLR7. Nat Med. 2005;11:263-270.
22. Bridge AJ, Pebernard S, Ducraux A, Nicoulaz AL,

Iggo R. Induction of an interferon response by RNAi vectors in mammalian cells. Nat Genet. 2003;34:263-264.

23. Sledz CA, Holko M, de Veer MJ, Silverman RH, Williams BR. Activation of the interferon system by short-interfering RNAs. Nat Cell Biol. 2003;5: 834-839.
24. Carr JM, Hocking H, Li P, Burrell CJ. Rapid and efficient cell-to-cell transmission of human immunodeficiency virus infection from monocyte-derived macrophages to peripheral blood lymphocytes. Virology. 1999;265:319-329.
25. Garcia-Blanco MA, Cullen BR. Molecular basis of latency in pathogenic human viruses. Science. 1991;254:815-820.
26. McCune JM. Viral latency in HIV disease. Cell. 1995;82:183-188.
27. Finzi D, Siliciano RF. Viral dynamics in HIV-1 infection. Cell. 1998;93:665-671.
28. Chun TW, Stuyver L, Mizell SB, et al. Presence of an inducible HIV-1 latent reservoir during highly active antiretroviral therapy. Proc Natl Acad Sci U S A. 1997;94:13193-13197.
29. Finzi D, Hermankova M, Pierson T, et al. Identification of a reservoir for HIV-1 in patients on highly active antiretroviral therapy. Science. 1997; 278:1295-1300.
30. Wong JK, Hezareh M, Gunthard HF, et al. Recovery of replication-competent HIV despite prolonged suppression of plasma viremia. Science. 1997;278:1291-1295.
31. Chun TW, Engel D, Mizell SB, Ehler LA, Fauci AS. Induction of HIV-1 replication in latently infected $CD4^+$ T cells using a combination of cytokines. J Exp Med. 1998;188:83-91.
32. Boden D, Pusch O, Lee F, Tucker L, Ramratnam B. Human immunodeficiency virus type 1 escape from RNA interference. J Virol. 2003;77:11531-11535.
33. Das AT, Brummelkamp TR, Westerhout EM, et al. Human immunodeficiency virus type 1 escapes from RNA interference-mediated inhibition. J Virol. 2004;78:2601-2605.
34. Moore JP, Kitchen SG, Pugach P, Zack JA. The CCR5 and CXCR4 coreceptors—central to understanding the transmission and pathogenesis of human immunodeficiency virus type 1 infection. AIDS Res Hum Retroviruses. 2004;20:111-126.
35. Aquaro S, Calio R, Balzarini J, Bellocchi MC, Garaci E, Perno CF. Macrophages and HIV infection: therapeutical approaches toward this strategic virus reservoir. Antiviral Res. 2002;55:209-225.
36. Capodici J, Kariko K, Weissman D. Inhibition of HIV-1 infection by small interfering RNA-mediated RNA interference. J Immunol. 2002; 169:5196-5201.
37. Dave RS, Pomerantz RJ. Antiviral effects of human immunodeficiency virus type 1-specific small interfering RNAs against targets conserved in select neurotropic viral strains. J Virol. 2004;78: 13687-13696.
38. Stevenson M. Dissecting HIV-1 through RNA interference. Nat Rev Immunol. 2003;3:851-858.
39. Cullen BR. HIV-1 auxiliary proteins: making connections in a dying cell. Cell. 1998;93:685-692.
40. Loetscher P, Uguccioni M, Bordoli L, et al. CCR5 is characteristic of Th1 lymphocytes. Nature. 1998;391:344-345.
41. Luther SA, Cyster JG. Chemokines as regulators of T cell differentiation. Nat Immunol. 2001;2:102-107.

nature immunology

Negative regulation of interferon-regulatory factor 3–dependent innate antiviral response by the prolyl isomerase Pin1

Tatsuya Saitoh[1], Adrian Tun-Kyi[2,8], Akihide Ryo[3,8], Masahiro Yamamoto[4], Greg Finn[2], Takashi Fujita[5], Shizuo Akira[4,6], Naoki Yamamoto[1,7], Kun Ping Lu[2] & Shoji Yamaoka[1]

Recognition of double-stranded RNA activates interferon-regulatory factor 3 (IRF3)–dependent expression of antiviral factors. Although the molecular mechanisms underlying the activation of IRF3 have been studied, the mechanisms by which IRF3 activity is reduced have not. Here we report that activation of IRF3 is negatively regulated by the peptidyl-prolyl isomerase Pin1. After stimulation by double-stranded RNA, induced phosphorylation of the Ser339–Pro340 motif of IRF3 led to its interaction with Pin1 and finally polyubiquitination and then proteasome-dependent degradation of IRF3. Suppression of Pin1 by RNA interference or genetic deletion resulted in enhanced IRF-3-dependent production of interferon-β, with consequent reduction of virus replication. These results elucidate a previously unknown mechanism for controlling innate antiviral responses by negatively regulating IRF3 activity via Pin1.

The innate immune response is an important, evolutionarily conserved mechanism that protects the host from both viral and microbial infections[1–3]. Increasing evidence has shown the importance of pattern-recognition receptors in immune responses after viral and microbial infection by invading pathogens[3]. Toll-like receptor 3 (TLR3) detects extracellular viral double-stranded RNA (dsRNA) internalized into the endosomes, whereas retinoic acid–inducible gene I (RIG-I), a DExD/H box RNA helicase containing a caspase-recruitment domain, detects intracellular viral dsRNA[3–5]. TLR4, in contrast, recognizes microbial components such as bacterial lipopolysaccharide (LPS)[6]. Engagement of any of those receptors triggers rapid production of type I interferon (IFN-αβ) and thus establishes the innate immune status against infectious agents[3,5,7].

Interferon-regulatory factor 3 (IRF3), a ubiquitously expressed transcription factor, is responsible for the primary induction of IFN-β and is important in the establishment of innate immunity in response to either viral or microbial infection[1–3]. After the detection of pathogens, IRF3 is phosphorylated on multiple phosphorylation acceptor (phospho-acceptor) sites, forms homodimers and then translocates to the nucleus, where it binds to the interferon stimulation–response elements of target genes, as well as the positive regulatory domain III-I in the IFN-β promoter[1–3]. The mechanisms underlying the phosphorylation-induced activation of IRF3 have been the subject of many extensive studies[8–16]. The substitution of alanine for either the Ser385 or Ser386 residue of IRF3 abolishes its activation[8,9]. Additionally, phosphorylation of Ser386 on IRF3 is induced by TLR3 engagement and by viral infection and only for IRF3 dimers[9]. The importance of five critical serine or threonine residues of IRF3 (Ser396, Ser398, Ser402, Thr404 and Ser405) for its activation has been demonstrated[10,11]. Notably, the substitution of alanine for all five amino acids abrogates the function of IRF3 to activate transcription, whereas aspartic acid substitutions result in a constitutively active protein. Those published data demonstrate that phosphorylation of both C-terminal phospho-accepter clusters (Ser385-Ser386 and Ser396-Ser398-Ser402-Thr404-Ser405) is important for the activation of IRF3. Other studies have also shown that two IκB kinase (IKK)–like kinases, TBK1-NAK and IKK-*i*–IKKε, are required for the activation of IRF3 by inducing the phosphorylation of its two C-terminal phospho-acceptor clusters and thus are essential in the expression of type I interferon[14–17]. Phosphorylation-dependent post-translational modifications of IRF3 are therefore crucial for regulating the function of IRF3.

Pin1 is a peptidyl-prolyl isomerase that via its WW domain (with two conserved tryptophan residues) specifically recognizes phosphorylated serine or threonine residues followed by proline and then catalyzes a conformational change of the bound substrate in a

[1]Department of Molecular Virology, Graduate School of Medicine, Tokyo Medical and Dental University, Tokyo 113-8519, Japan. [2]Cancer Biology Program, Division of Hematology/Oncology, Department of Medicine, Beth Israel Deaconess Medical Center, Harvard Medical School, Boston, Massachusetts 02115, USA. [3]Department of Pathology, Yokohama City University, Yokohama, Kanagawa 236-0004, Japan. [4]Department of Host Defense, Research Institute for Microbial Diseases, Osaka University, Osaka 565-0871, Japan. [5]Laboratory of Molecular Genetics, Institute for Virus Research, Kyoto University, Kyoto 606-8507, Japan. [6]ERATO, Japan Science and Technology Agency, Osaka 565-0871, Japan. [7]AIDS Research Center, National Institute of Infectious Diseases, Tokyo 162-8640, Japan. [8]These authors contributed equally to this work. Correspondence should be addressed to S.Y. (shojmmb@tmd.ac.jp) or A.R. (aryo@yokohama-cu.ac.jp).

Received 23 January; accepted 5 April; published online 14 May 2006; doi:10.1038/ni1347

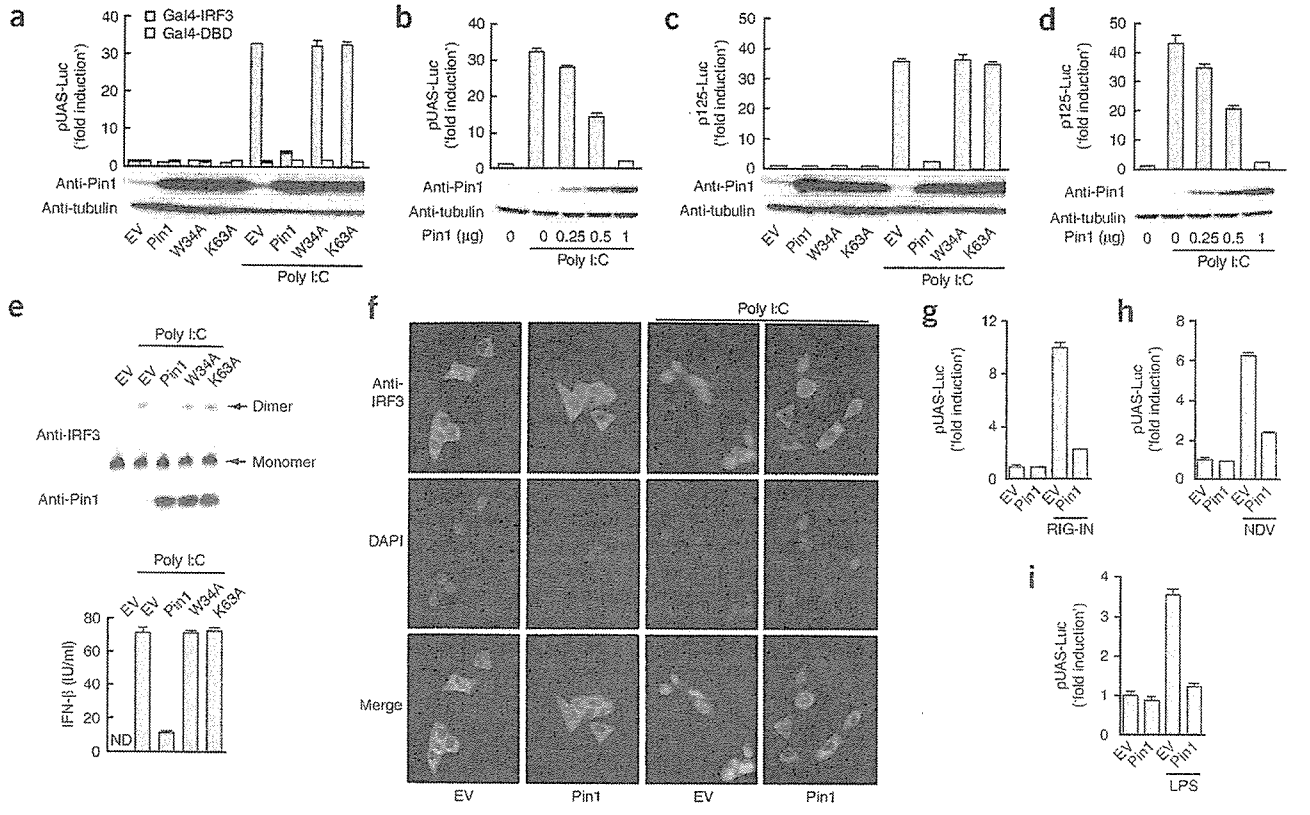

Figure 1 Pin1 suppresses IRF3-dependent transcriptional activation. (**a–d**) Luciferase assay (above) and immunoblot (below) of lysates from 293-TLR3 cells transfected with pEF1-lacZ and either the Gal4-site luciferase reporter pUAS-Luc (**a,b**) or the IFN-β promoter reporter p125-Luc (**c,d**), transiently expressing empty vector (EV), wild-type Pin1 or Pin1 mutants and either Gal4-IRF3 or Gal4-DBD (control; **a,c**) or transiently expressing various amounts of wild-type Pin1 (below lanes; **b,d**), and then stimulated with poly(I)•poly(C) (poly I:C). Luciferase activity is normalized to β-galactosidase activity; results are means ± s.d. from three separate transfections. (**e**) Immunoblots of endogenous IRF3 dimer detected by native PAGE (top) and Pin1 expression detected by SDS-PAGE (middle) in 293-TLR3 cells transiently expressing empty vector, wild-type Pin1 or Pin1 mutants and left unstimulated (far left) or stimulated for 3 h with poly(I)•poly(C). Bottom, ELISA of IFN-β secreted into the culture supernatant. ND, not detected. (**f**) Immunohistochemistry to detect endogenous IRF3 (green) in 293-TLR3neo^r cells stably expressing Pin1 with or without poly(I)•poly(C) stimulation. Cell nuclei are blue (DAPI, 4,6-diamidino-2-phenylindole). Original magnification, ×40. (**g**) Luciferase assay of lysates prepared from 293 cells at 36 h after transfection with pEF1-lacZ and pUAS-Luc and expressing Pin1 and Gal4-IRF3 with or without the RIG-I N-terminal caspase-recruitment domain (RIG-IN). (**h,i**) Luciferase assay of lysates from 293 cells (**h**) or U373-CD14 cells (**i**) transfected with pEF1-lacZ and pUAS-Luc, transiently expressing Pin1 and Gal4-IRF3, and then infected with NDV (**h**) or treated with LPS (**i**). Data are representative of two independent experiments.

phosphorylation-dependent way[18,19]. By that mechanism, Pin1 has been shown to regulate the stability and or localization of its substrates during transcriptional activation, cell cycle progression and cell death, and deregulated expression or loss of function of Pin1 leads to the progression of important human diseases such as cancer and Alzheimer disease[18,20–28]. However, a regulatory function for Pin1 in the host defense against infectious agents and associated signal transduction pathways has not been reported before to our knowledge. Published findings showing that post-translational modification of IRF3 by phosphorylation controls the IRF3 activity prompted us to assess the involvement of Pin1 in regulating IRF3 signaling.

RESULTS

Pin1 suppresses IRF3-dependent transcriptional activation

A well characterized stimulation for IRF3 activation is TLR3 engagement with the synthetic dsRNA poly(I)•poly(C)[7,14,29,30]. We therefore used that mode of activating IRF3 to investigate possible involvement of Pin1 in regulating the activity of IRF3. Reporter gene assays using a yeast transcription factor Gal4–IRF3 fusion protein showed that exogenous expression of wild-type Pin1 inhibited poly(I)•poly(C)-induced IRF3-dependent transcriptional activation in a dose-dependent way, but expression of its WW domain mutant (W34A) or peptidyl-prolyl isomerase domain mutant (K63A) did not (**Fig. 1a,b**). That result indicated that functional WW and peptidyl-prolyl isomerase domains of Pin1 are required for the regulation of IRF3 signaling. Similarly, exogenous expression of wild-type Pin1 suppressed TLR3-mediated, IRF3-dependent activation of the IFN-β promoter and reduced IFN-β secretion in culture supernatants (**Fig. 1c–e**). We next addressed whether Pin1 affects the dimerization and nuclear localization of endogenous IRF3 that normally occurs after poly(I)•poly(C) stimulation. Native gel electrophoresis and immunoblot of cell lysates after poly(I)•poly(C) stimulation showed that exogenous Pin1 expression produced a considerable reduction in the activated dimer form of IRF3 (**Fig. 1e**). Immunocytochemical analyses confirmed that Pin1 overexpression decreased the amount of nuclear IRF3 (**Fig. 1f**).

We next assessed if exogenous Pin1 expression would inhibit IRF3 signaling induced by RIG-I-mediated detection of RNA virus infection or by LPS stimulation of TLR4. In agreement with published results[5], we found that IRF3-dependent transcriptional activation by the N-terminal caspase-recruitment domain of RIG-I was inhibited by exogenously expressed Pin1 (**Fig. 1g**). In addition, expression of Pin1 inhibited Newcastle disease virus (NDV)–induced IRF3-dependent

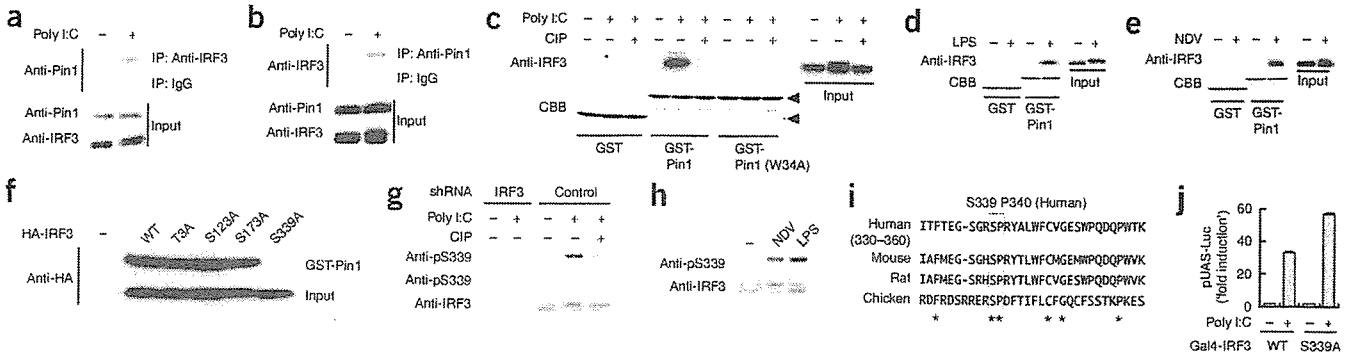

Figure 2 Pin1 interacts with IRF3 through its phosphorylated Ser339–Pro340 motif. (**a**,**b**) Immunoprecipitation (IP) and immunoblot of lysates from 293-TLR3 cells stimulated for 2 h with poly(I)•poly(C), analyzed with either polyclonal anti-IRF3 and anti-Pin1 (**a**) or anti-Pin1 and anti-IRF3 (**b**) or control immunoglobulin G (IgG). (**c**) PAGE and immunoblot with anti-IRF3 of affinity-purified lysates from 293-TLR3 cells stimulated for 2 h with poly(I)•poly(C) or left untreated. Lysates were left untreated or were treated with calf intestinal alkaline phosphatase (CIP), followed by incubation with GST, GST-Pin1 or GST-Pin1 W34A. Recombinant GST proteins (arrowheads) are visualized by Coomassie brilliant blue staining (CBB). (**d**,**e**) GST-Pin1 affinity assay of lysates from U373-CD14 cells stimulated for 2 h with LPS (**d**) or from 293 cells infected for 12 h with NDV or left untreated (**e**). (**f**) GST-Pin1 affinity assay of lysates from 293-TLR3 cells transfected with hemagglutinin-tagged wild-type IRF3 (WT) or various IRF3 mutants, stimulated with poly(I)•poly(C). (**g**) Immunoblot of lysates from U373-CD14 cells infected with a retroviral IRF3-specific or control shRNA construct and selected with puromycin. Cell pools were stimulated with poly(I)•poly(C), then lysates were treated with calf intestinal alkaline phosphatase and were analyzed by PAGE and immunoblot with anti–phospho-Ser339 (Anti-pS339), preincubated with phosphorylated (middle) or unphosphorylated (top) Ser339 peptide. Bottom, immunoblot with anti-IRF3. (**h**) PAGE and immunoblot of lysates from U373-CD14 cells treated with NDV or LPS, analyzed with anti–phospho-Ser339. (**i**) Amino acid alignment of the C-terminal regions of human, mouse, rat and chicken IRF3. *, amino acid residues conserved among the four species; boxed amino acid residues correspond to human Ser339 and Pro340. (**j**) Luciferase assay of lysates from 293-TLR3 cells transfected with pEF1-lacZ and pUAS-Luc and expressing either wild-type Gal4-IRF3 (WT) or the Gal4-IRF3 S339A mutant (S339A), stimulated for 9 h with poly(I)•poly(C). Data are representative of two independent experiments.

transcriptional activation, which is mediated by RIG-I (ref. 5; **Fig. 1h**). Finally, expression of Pin1 also suppressed TLR4-mediated IRF3-dependent transcriptional activation (**Fig. 1i**). These results strongly suggested that Pin1 is a negative regulator of a transcriptional activator of IFN-β and acts on a mediator shared by three independent pathways of IRF3 activation, indicating direct negative regulation of IRF3 itself.

Pin1 interacts with IRF3 in a phosphorylation-dependent way

Because Pin1 has been reported to regulate a subset of transcription factors[18], we determined if it physically interacts with IRF3. Immunoprecipitation followed by immunoblot analysis showed that poly(I)•poly(C) stimulation induced interaction of endogenous Pin1 with endogenous IRF3 *in vivo* (**Fig. 2a**,**b**). Glutathione *S*-transferase (GST) affinity assays further demonstrated an *in vitro* interaction between purified GST-Pin1 and endogenous IRF3 (**Fig. 2c**), and pretreatment of cell lysates with calf intestinal alkaline phosphatase abolished the interaction, indicating that phosphorylation is a prerequisite for the Pin1-IRF3 interaction. Consistent with that, the WW domain mutant of Pin1 (W34A) failed to interact with IRF3. LPS stimulation and NDV infection also induced the interaction of Pin1 with IRF3 (**Fig. 2d**,**e**).

We next sought to identify the specific Ser-Pro or Thr-Pro residues of IRF3 targeted by Pin1. The phospho-accepter residues required for IRF3 activation do not contain the Ser-Pro or Thr-Pro motif required for interaction with Pin1 (refs. 8–16). There are five Ser-Pro or Thr-Pro sites in human IRF3, and four of those (Thr3, Ser 123, Ser 173 and Ser339) are conserved between human and mouse. We analyzed mutants with site-directed substitution of each potential Pin1-binding site of IRF3 (substitution of alanine for serine or threonine) for Pin1 binding after poly(I)•poly(C) treatment; only the S339A substitution substantially disrupted the interaction between IRF3 and Pin1 (**Fig. 2f**). Immunoblot analysis with antibodies raised against an IRF3 peptide phosphorylated at Ser339 (anti–phospho-Ser339) demonstrated that this Ser residue of endogenous IRF3 was phosphorylated after stimulation with poly(I)•poly(C), LPS or NDV (**Fig. 2g**,**h**). Preincubation of anti–phospho-Ser339 with the phosphorylated peptide blocked detection of phosphorylated IRF3, but preincubation with the unphosphorylated peptide did not, establishing the specificity of the antibody (**Fig. 2g**). Suppression of endogenous IRF3 expression by RNA interference or by treatment of cell lysates with alkaline phosphatase diminished the immunoreactivity of anti–phospho-Ser339, indicating that it recognizes phosphorylated IRF3 (**Fig. 2g**). Notably, the amino acid residues corresponding to Ser339-Pro340 in human IRF3 are highly conserved among other species, such as mouse, rat and chicken (**Fig. 2i**), suggesting the importance of this Ser-Pro motif. At present, the kinase responsible for Ser339 phosphorylation remains unknown. Although phosphorylation at Ser396, which is reported to be mediated by TBK1 and IKK-*i*[9,15,16], reached a peak 1 h after stimulation with poly(I)•poly(C) or LPS, phosphorylation at Ser339 was detected several hours later (**Supplementary Fig. 1** online). Loss-of-function experiments using an RNA-interference strategy demonstrated involvement of TBK1 and IKK-*i* in the phosphorylation of Ser339 as well as Ser396 after poly(I)•poly(C) stimulation (**Supplementary Fig. 2** online). However, we do not have evidence for direct phosphorylation of Ser339 by these IKK-related kinases and cannot exclude the possibility that phosphorylation of the C-terminal phospho-accepter clusters by TBK1 and IKK-*i* somehow facilitates subsequent phosphorylation of Ser339 by another kinase. We confirmed the biological consequences of Ser339 phosphorylation by reporter gene assay. The S339A substitution augmented the activation of the reporter gene by poly(I)•poly(C) stimulation (**Fig. 2j**). These results collectively suggest that phosphorylation of IRF3 Ser339 and subsequent interaction with Pin1 are important for the negative regulation of IRF3 signaling.

Pin1 destabilizes activated IRF3

The interaction of Pin1 and IRF3 leading to suppression of IRF3 activity prompted us to examine whether Pin1 regulates IRF3

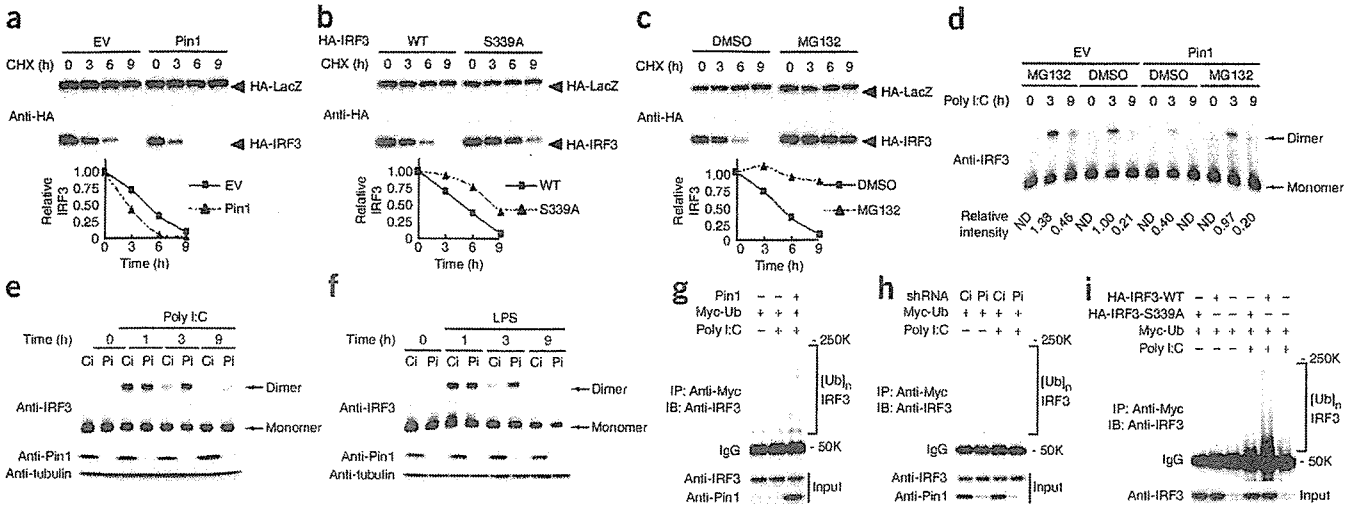

Figure 3 Pin1 regulates the stability of IRF3. (**a**) Immunoblot of lysates from 293-TLR3 cells transiently expressing Pin1, HA-lacZ and HA-IRF3, stimulated with poly(I)•poly(C) and then cultured in the presence of cycloheximide (CHX; time, above lanes). Expression of HA-IRF3 is normalized to that of HA-lacZ (graphed below). (**b**) Immunoblot of lysates from 293-TLR3 cells transiently expressing wild-type HA-IRF3 (WT) and HA-lacZ or HA-IRF3 S339A (S339A) and HA-lacZ and then treated as described in **a**. (**c**) Immunoblot of lysates from 293-TLR3 cells transiently expressing HA-IRF3 and HA-lacZ and then stimulated with poly(I)•poly(C) in the presence of cycloheximide and either DMSO (dimethyl sulfoxide) or MG132 (10 μM). (**d**) Native PAGE and immunoblot with anti-IRF3 of lysates from 293-TLR3 cells transiently expressing Pin1 and stimulated with poly(I)•poly(C) (time, above lanes) in the presence or absence (DMSO) of 10 μM MG132. Bottom, relative amount of IRF3 dimer. (**e**,**f**) Native PAGE and immunoblot with anti-IRF3 of lysates from U373-CD14 cells infected with a retroviral control (Ci) or Pin1-specific (Pi) shRNA construct and stimulated (time, above lanes) with poly(I)•poly(C) (**e**) or LPS (**f**). (**g**) Immunoprecipitation with anti-Myc and immunoblot (IB) with anti-IRF3 of whole-cell lysates from 293-TLR3 cells expressing Myc-tagged ubiquitin (Myc-Ub) and stimulated with poly(I)•poly(C) in the presence of MG132. $[Ub]_n$, polyubiquitination. (**h**) Immunoprecipitation with anti-Myc and immunoblot with anti-IRF3 of lysates from 293 cells infected with retroviral control or Pin1-specific shRNA, transiently expressing human TLR3 and Myc-tagged ubiquitin and stimulated with poly(I)•poly(C) in the presence of MG132. (**i**) Immunoprecipitation with anti-Myc and immunoblot with anti-IRF3 of whole-cell lysates from 293-TLR3 cells transiently expressing various proteins (above lanes) and stimulated with poly(I)•poly(C) in the presence of MG132. Data are representative of two independent experiments.

protein stability. Because IRF3 is highly stable in the steady state[31] (data not shown), we induced IRF3 activation by stimulation with poly(I)•poly(C). After activation with poly(I)•poly(C), IRF3 degraded more rapidly in 293 cell cultures stably expressing human TLR3 ('293-TLR3' cells) expressing exogenous Pin1 (**Fig. 3a**), and the IRF3 S339A mutant, which was defective in Pin1 binding, had a slower turnover than that of wild-type IRF3 (**Fig. 3b**). In the presence of the proteasome inhibitor MG132, IRF3 demonstrated considerably increased stability (**Fig. 3c**), suggesting that a proteasome-dependent mechanism underlies the negative regulation of IRF3. Our finding that Pin1 reduced the homodimer of IRF3 (**Fig. 1e**), in combination with these data demonstrating that turnover of IRF3 may involve a proteasome-dependent process, led us to determine how MG132 and/or Pin1 influences the status of the activated dimer form of IRF3 induced by poly(I)•poly(C) stimulation. Treatment with MG132 substantially increased the amount of IRF3 dimer, whereas the addition of exogenous Pin1 expression reduced the amount of IRF3 dimer (**Fig. 3d**). The addition of MG132 reversed the suppressive effects of Pin1 on IRF3 (**Fig. 3d**).

To verify the function of endogenous Pin1 in IRF3 signaling, we generated a short hairpin RNA (shRNA) expression construct capable of 'knocking down' Pin1 expression. Stable expression of Pin1-specific shRNA effectively reduced the amount of endogenous Pin1 but did not alter the expression of α-tubulin (**Fig. 3e,f**). Native PAGE coupled with immunoblot analysis showed that the suppression of endogenous Pin1 expression greatly increased IRF3 dimers induced by poly(I)•poly(C) or LPS at later time points but not at 1 h after stimulation (**Fig. 3e,f**). These results indicated that Pin1 'preferentially' promotes proteasome-dependent degradation of activated IRF3.

Ubiquitination-dependent degradation of transcription factors is an important mechanism for the termination of transcriptional activation[32]. Because we had found that proteasome inhibition delayed the degradation of IRF3 (**Fig. 3c**), we determined whether IRF3 is ubiquitinated. Immunoprecipitation of ubiquitin followed by immunoblot analysis for IRF3 demonstrated that polyubiquitination of IRF3 was induced by poly(I)•poly(C) stimulation (**Fig. 3g**) and that polyubiquitination was augmented by Pin1 expression and abrogated by expression of Pin1-specific shRNA (**Fig. 3g,h**). Consistent with the finding that Pin1 facilitated IRF3 degradation after poly(I)•poly(C) stimulation (**Fig. 3a**), the S339A mutant of IRF3 was less susceptible to polyubiquitination than was wild-type protein (**Fig. 3i**). These results indicated that Pin1 regulates ubiquitination and proteasome-mediated proteolysis of IRF3.

Endogenous Pin1 regulates TLR3-mediated IFN-β production

We next investigated the function of endogenous Pin1 in dsRNA-induced, IRF3-dependent transcriptional activation. As anticipated, expression of Pin1-specific shRNA enhanced IRF3-dependent transcriptional activation and thus enhanced activation of the IFN-β promoter triggered by the engagement of TLR3 (**Fig. 4a,b**). In contrast, expression of Pin1-specific shRNA did not affect TLR3-mediated activation of NF-κB, a transcription factor also involved in IFN-β production (**Supplementary Fig. 3** online). Moreover, expression of a second Pin1-specific shRNA also augmented IRF3-dependent reporter gene activation, and complementation with mouse Pin1, which does not contain the human Pin1 shRNA target sequence, reversed the effects on IRF3-dependent transcriptional activation (**Supplementary Fig. 4** online). To investigate the temporal regulation of IRF3-dependent transcription by Pin1, we used a

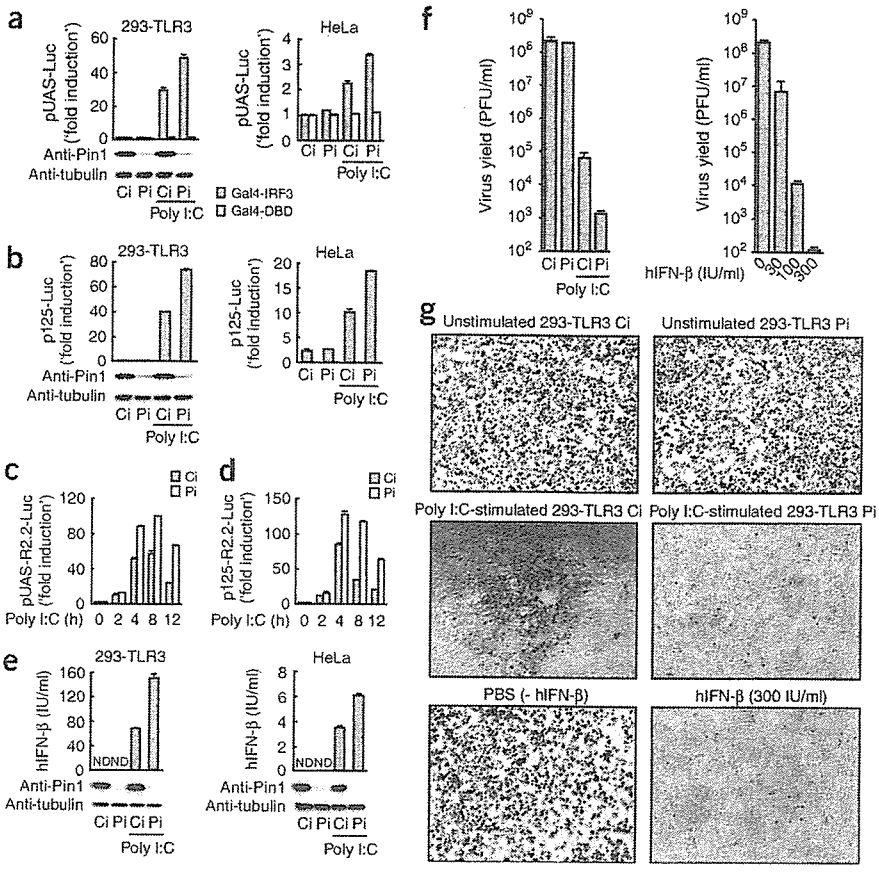

Figure 4 Endogenous Pin1 negatively regulates TLR3-mediated IRF3-dependent transcriptional activation and IFN-β production. (**a–d**) Luciferase assay of lysates from 293-TLR3 cells (**a–d**) and HeLa cells (**a,b**, right) transfected with pEF1-lacZ and pUAS-Luc (**a**), p125-Luc (**b**), pUAS-R2.2-Luc (**c**) or p125-R2.2-Luc (**d**) and transiently expressing control or Pin1-specific shRNA (**a–d**) and Gal4-IRF3 (**a,c**). Cells were stimulated with poly(I)•poly(C) for 9 h (**a,b**) or for various times (horizontal axes; **c,d**); relative luciferase activities are presented as in **Figure 1**. Expression of Pin1 in 293-TLR3 cells was verified by immunoblot (**a, b**, bottom). (**e**) ELISA of human IFN-β (hIFN-β) secretion from either 293-TLR3 cells transiently expressing control or Pin1 shRNA (left) or HeLa cells infected with retroviruses expressing either control or Pin1 shRNA (right), analyzed after stimulation for 12 h with poly(I)•poly(C). Data are means ± s.d. from three separate samples. (**f**) VSV production (in plaque-forming units (PFU)/ml) 24 h after infection of Vero cells previously treated with supernatants from 293-TLR3 cells transiently expressing control or Pin1 shRNA and stimulated for 12 h with poly(I)•poly(C) (left) or with various concentrations of human IFN-β (right). (**g**) Phase-contrast micrographs of VSV-infected Vero cells. Dead cells (round shape) are detached from the culture dish. Original magnification, ×20. Data are representative of two independent experiments.

rapid-response luciferase reporter gene. Real-time reporter gene assays showed that suppression of endogenous Pin1 expression substantially prolonged both IRF3-dependent transcription and IFN-β promoter activation after poly(I)•poly(C) stimulation (**Fig. 4c,d**). Consistent with the inhibitory effects of Pin1 on the IFN-β promoter, expression of Pin1-specific shRNA but not that of control shRNA increased the production of IFN-β induced by poly(I)•poly(C) (**Fig. 4e**). Because exogenous expression of Pin1 greatly reduced the production of a potent antiviral secreted factor (IFN-β) from poly(I)•poly(C)-stimulated 293-TLR3 cells (**Supplementary Fig. 5** online), we assessed if endogenous Pin1 was sufficient to induce the same regulation. Culture supernatants of poly(I)•poly(C)-stimulated 293-TLR3 cells expressing Pin1-specific shRNA had approximately 50 times more antiviral activity than that of supernatant of cells expressing control shRNA (**Fig. 4f**); moreover, this amount of secreted antiviral factor was sufficient to fully protect fresh cells from productive infection by vesicular stomatitis virus (VSV; **Fig. 4g**). These results indicated that Pin1 is involved in terminating IRF3 signaling triggered after TLR3 engagement with activating ligand and thus Pin1 regulates the expression of IRF3 target genes relevant to the innate antiviral response. However, unlike other negative regulators of TLR signaling whose expression is upregulated by stimulation[3], the expression of Pin1 protein was not substantially different after stimulation with poly(I)•poly(C) or IFN-β (**Supplementary Fig. 6** online).

Pin1 deficiency enhances IFN-β production induced by dsRNA

To assess the involvement of Pin1 in dsRNA-induced innate antiviral response in immune competent cells, we prepared bone marrow–derived macrophages from *Pin1*$^{-/-}$ or *Pin1*$^{+/+}$ mice. After being stimulated with poly(I)•poly(C), macrophages from *Pin1*$^{-/-}$ mice secreted more IFN-β than did wild-type cells (**Fig. 5a**). Those findings prompted us to determine if Pin1 also limits IFN-β induction *in vivo*. The amount of IFN-β produced after intraperitoneal injection of poly(I)•poly(C) was much greater in sera of *Pin1*$^{-/-}$ mice than in sera of similarly treated wild-type mice (**Fig. 5b**). These results provided

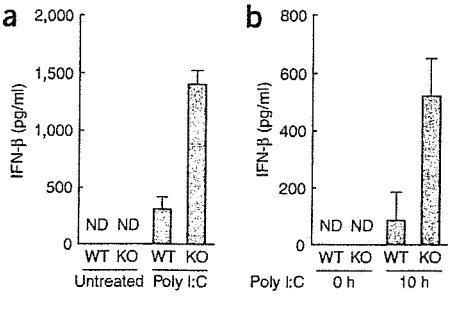

Figure 5 Pin1 deficiency enhances IFN-β production in response to dsRNA. (**a**) ELISA of IFN-β production from bone marrow–derived macrophages prepared from *Pin1*$^{+/+}$ (WT) or *Pin1*$^{-/-}$ (KO) mice; cells were left untreated or were stimulated for 8 h with poly(I)•poly(C) (25 μg/ml). Data are means ± s.d. of three independent experiments. (**b**) ELISA of IFN-β production in sera from *Pin1*$^{+/+}$ or *Pin1*$^{-/-}$ mice ($n = 3$ per group) injected intraperitoneally with 5 μg poly(I)•poly(C) per gram body weight. Sera were collected from each mouse before or 10 h after treatment. Error bars represent s.d.

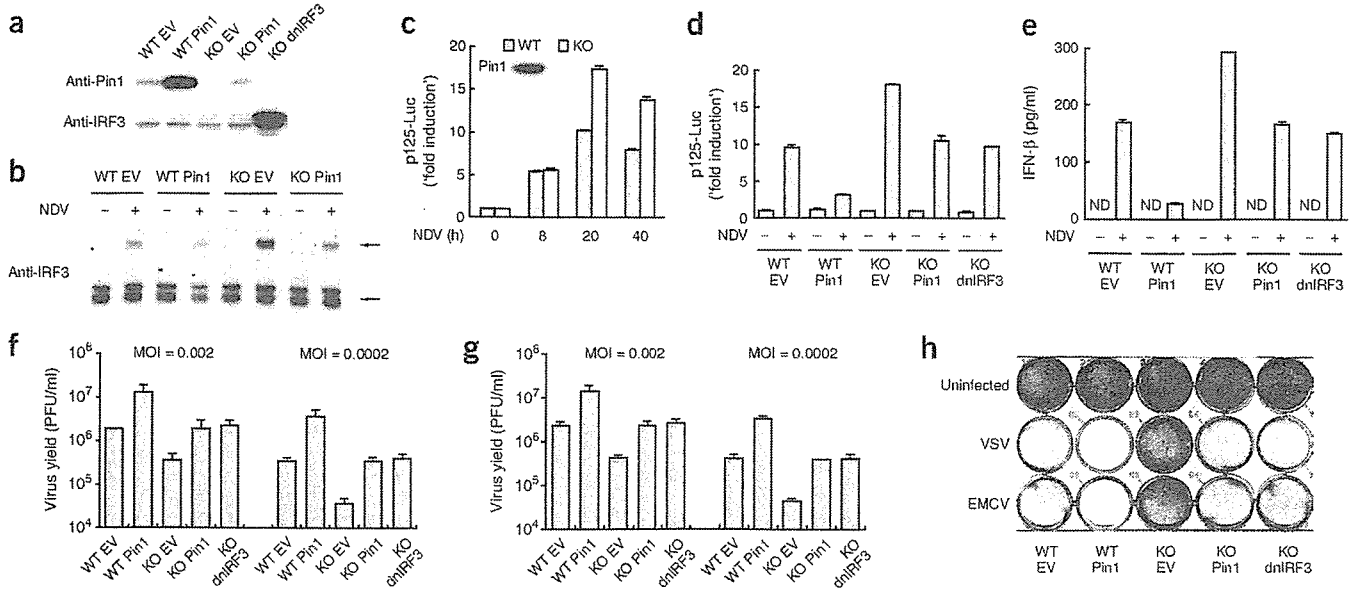

Figure 6 Pin1 regulates RIG-I-mediated IRF3 signaling and innate antiviral response. (**a**) Immunoblot with anti-Pin1 or anti-IRF3 of lysates from MEFs isolated from *Pin1*$^{+/+}$ (WT) or *Pin1*$^{-/-}$ (KO) mice infected with retroviruses expressing mouse Pin1 (WT-Pin1 or KO-Pin1) or hemagglutinin-tagged dominant negative IRF3 (KO dnIRF3) and selected with blasticidin S. (**b**) Native PAGE and immunoblot with anti-IRF3 of lysates from the MEFs described in **a**, infected for 30 h with NDV. Arrows (right margin) indicate IRF3 dimer (top) and monomer (bottom). (**c**) Luciferase assay of lysates from *Pin1*$^{+/+}$ or *Pin1*$^{-/-}$ MEFs transfected with p125-Luc and pEF1-lacZ and then infected with NDV (times, horizontal axis). Inset, immunoblot for Pin1. (**d**) Luciferase assay of lysates from the MEFs in **a**, transfected with p125-Luc and pEF1-lacZ and then infected for 20 h with NDV. (**e**) ELISA of IFN-β produced from the MEFs in **a**, infected for 40 h with NDV. (**f**,**g**) Virus production from the MEFs in **a**, infected with VSV (**f**) or EMCV (**g**) at a multiplicity of infection (MOI) of 0.002 (left) or 0.0002 (right). Virus yield in the supernatants at 20 h after infection was determined by plaque assay. (**h**) Amido black staining of the MEFs in **a**, infected for 20 h with VSV (MOI, 0.002) or EMCV (MOI, 0.002) but not killed; cells were fixed and then stained. Data are representative of two independent experiments.

genetic evidence that Pin1 regulates dsRNA-induced IFN-β production both *in vivo* and *in vitro*.

Pin1 regulates RIG-I-dependent antiviral cellular responses

To assess the involvement of Pin1 in the RIG-I-dependent antiviral cellular response, we used mouse embryonic fibroblasts (MEFs) isolated from *Pin1*$^{-/-}$ mice (**Fig. 6a**). Native PAGE coupled with immunoblot analysis showed that loss of Pin1 expression considerably increased the amount of IRF3 dimer (**Fig. 6b**). Complementation of *Pin1*$^{-/-}$ MEFs with expression of wild-type Pin1 normalized the IRF3 response to NDV infection, confirming that deregulated IRF3 activation in *Pin1*$^{-/-}$ MEFs was due to the loss of Pin1 expression. Reporter gene assays showed that the NDV-induced activation of the IFN-β promoter was enhanced at later time points in *Pin1*$^{-/-}$ MEFs compared with that of wild-type MEFs, an effect that was reversed by complementation with either wild-type Pin1 or a dominant negative mutant of IRF3 (**Fig. 6c,d**). Consistent with that finding, *Pin1*$^{-/-}$ MEFs demonstrated increased production of IFN-β after NDV infection (**Fig. 6e**). To demonstrate the specificity of Pin1 on IRF3 activation, we also evaluated NF-κB activation in *Pin1*$^{-/-}$ MEFs after NDV infection and found that it was only marginally affected by the absence of Pin1 (**Supplementary Fig. 3**). Finally, we noted that NDV infection weakly and transiently increased Pin1 protein expression (**Supplementary Fig. 6**).

We next sought to determine if Pin1 regulated replication of VSV and encephalomyocarditis virus (EMCV), as RIG-I-mediated IRF3 signaling is critical in restricting replication of these RNA viruses[5]. Consistent with the suppressive effects of Pin1 on RIG-I-mediated IRF3 signaling (**Fig. 1g,h**), exogenous expression of Pin1 increased the production of infectious VSV or EMCV in the culture supernatants of infected MEFs, whereas loss of Pin1 expression decreased it (**Fig. 6f,g**). Furthermore, the reduction of virus yield in *Pin1*$^{-/-}$ MEFs was reversed by the expression of a dominant negative form of IRF3. In agreement with those results, increased expression of Pin1 augmented virus-mediated cell killing, whereas loss of Pin1 expression protected cells (**Fig. 6h**). These results provide biological evidence that Pin1 acts as a negative regulator of RIG-I-mediated IRF3 signaling and thereby modulates the innate antiviral cellular response.

DISCUSSION

Studies have identified functions for Pin1 in a variety of pathological conditions[18]. Pin1 prevents the accumulation of hyperphosphorylated tau protein in the brain and thus protects neuronal cells from age-dependent degeneration[18,25]. However, increased expression of Pin1 has often been detected in many different neoplasms, such as breast cancer, and is also involved in the malignant transformation of cancer cells[18,24,33]. Here we have demonstrated that Pin1 is involved in the termination of IRF3-dependent transcriptional activation, which thereby provides negative regulation of the innate antiviral response against infection by RNA viruses. The results presented here suggest that increased expression of Pin1 suppresses the innate antiviral response and thus may allow the replication and persistence of infectious agents. If true, such a possibility could partly explain why cancer cells are more susceptible to lytic infection by VSV[34].

We have also demonstrated that the genetic absence or RNA interference-mediated suppression of Pin1 expression enhanced poly(I)•poly(C)-induced activation of IRF3 and consequent production of IFN-β. Because activation of IRF3 and production of IFN-β are known to mediate TLR-mediated toxicity[35,36] and because ectopic expression of a constitutively active IRF3 mutant induces cell death[37],